Coherent anti-Stokes Raman Scattering

Jean-Pierre Taran

Senior Advisor

ONERA

THE FRENCH AEROSPACE LAB

return on innovation

HOW IT STARTED

The challenge: measure aerodynamic and reactive flows

- **fast**
- **non-intrusively**
- **with good spatial resolution**

Measuring H_2 vibrational relaxation

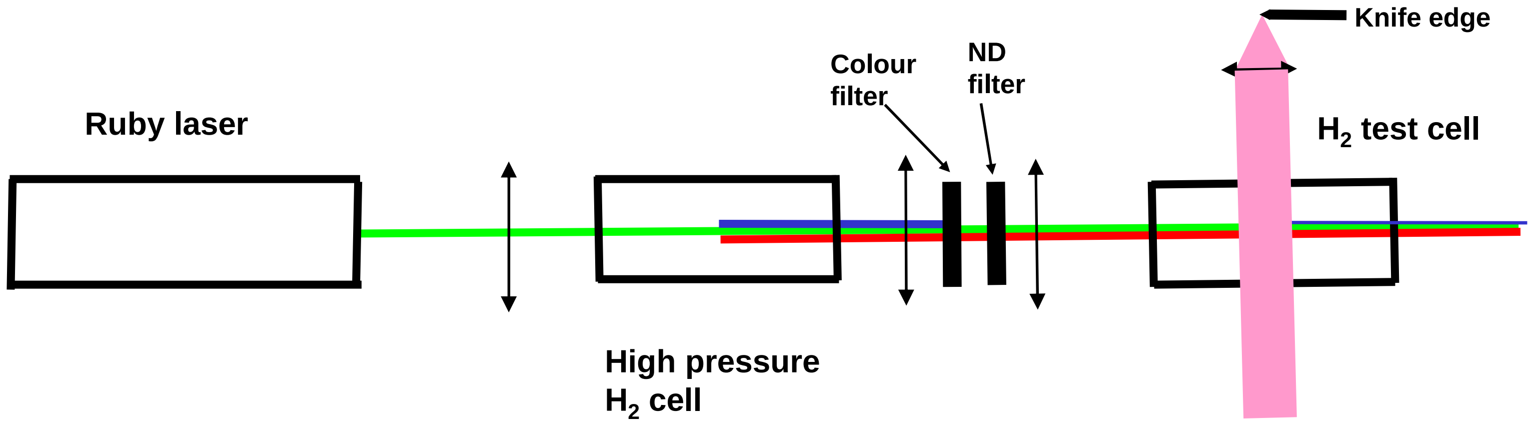

Audibert, Ducuing, Joffrin, Lukasik

First CARS setup at Onera

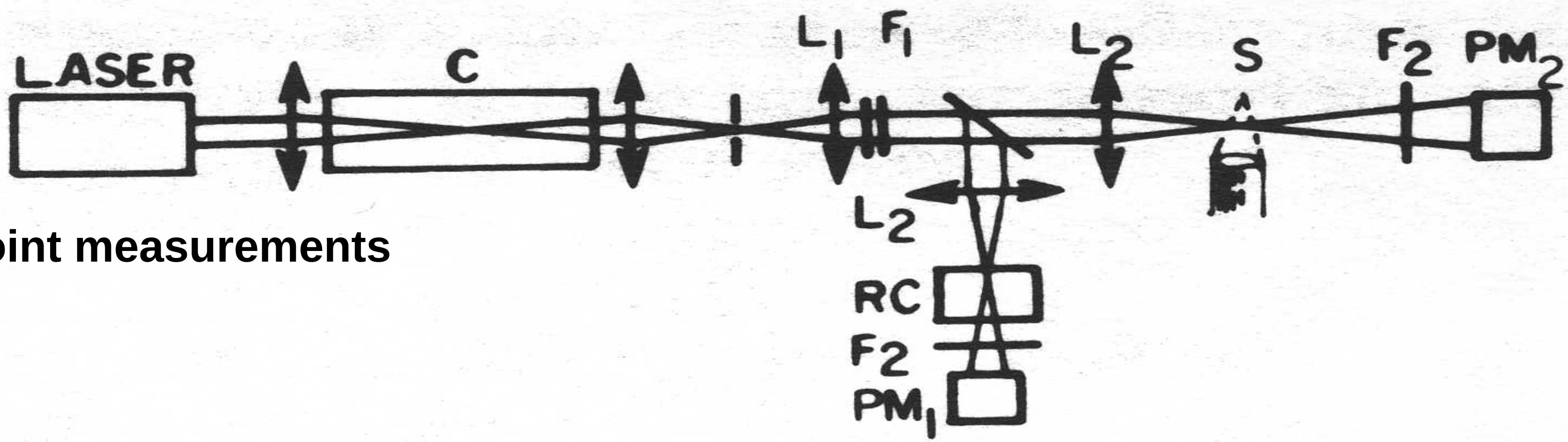

for point measurements

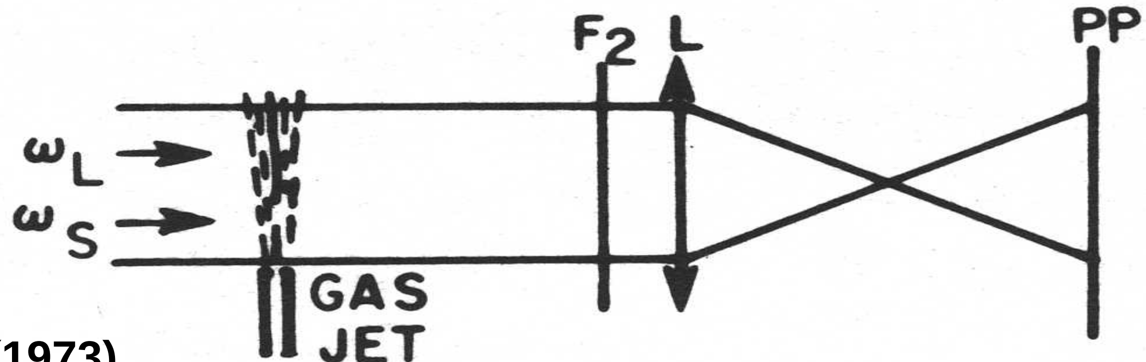

for visualisation

Régnier & Taran APL (1973)

CARS signal vs H_2 density in air

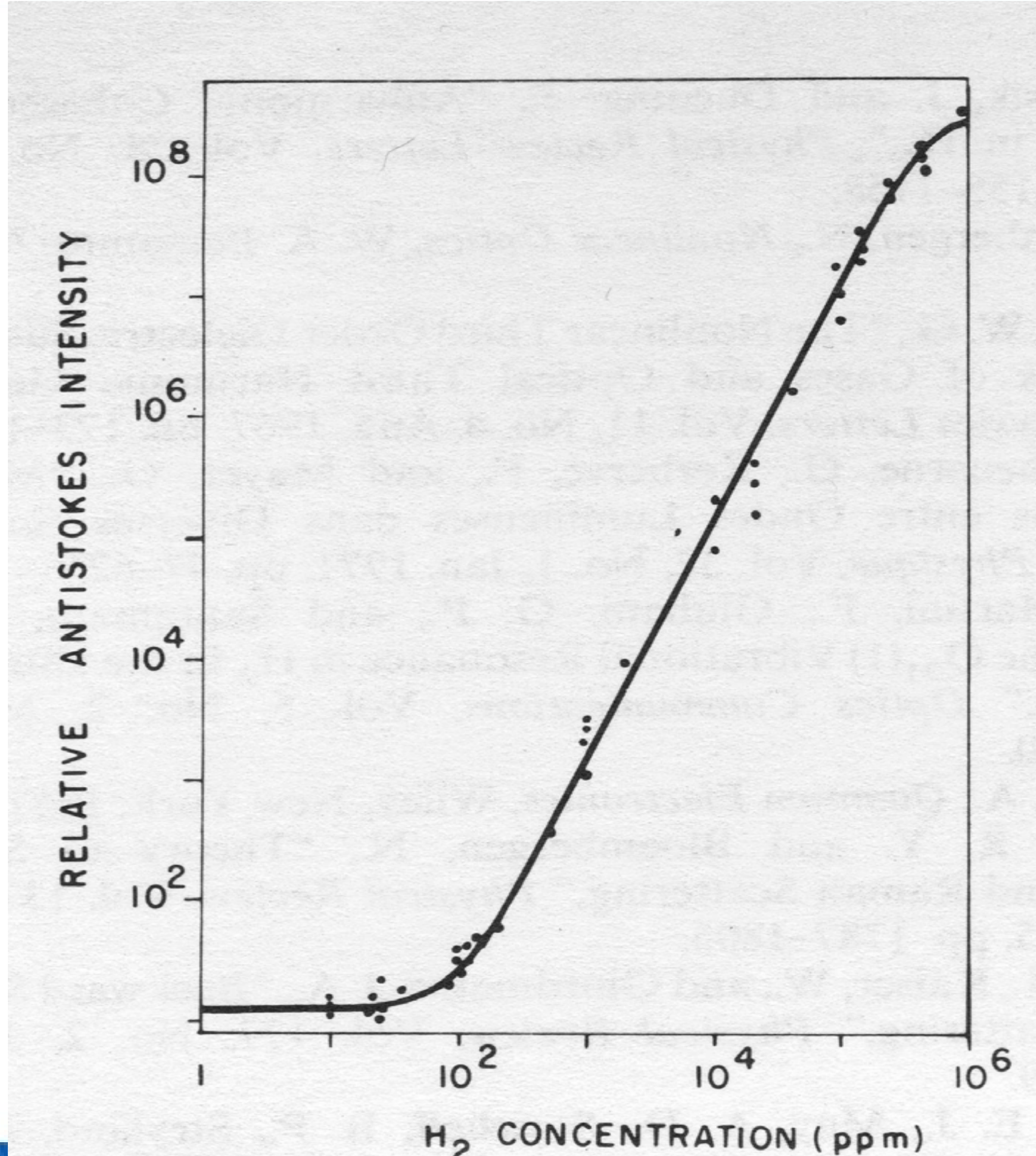

ONERA

Visualisation of supersonic H_2 jet

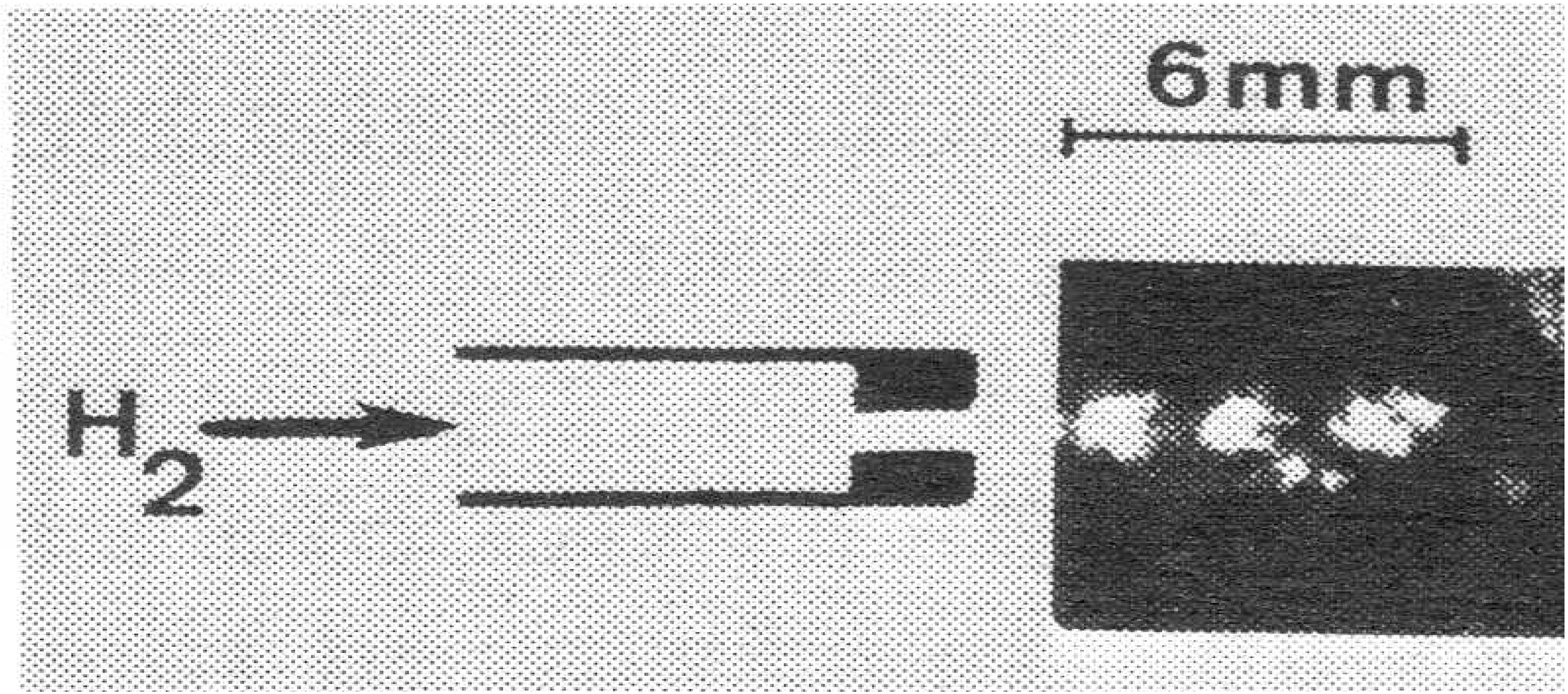

ONERA

H_2 distribution in horizontal Bunsen flame

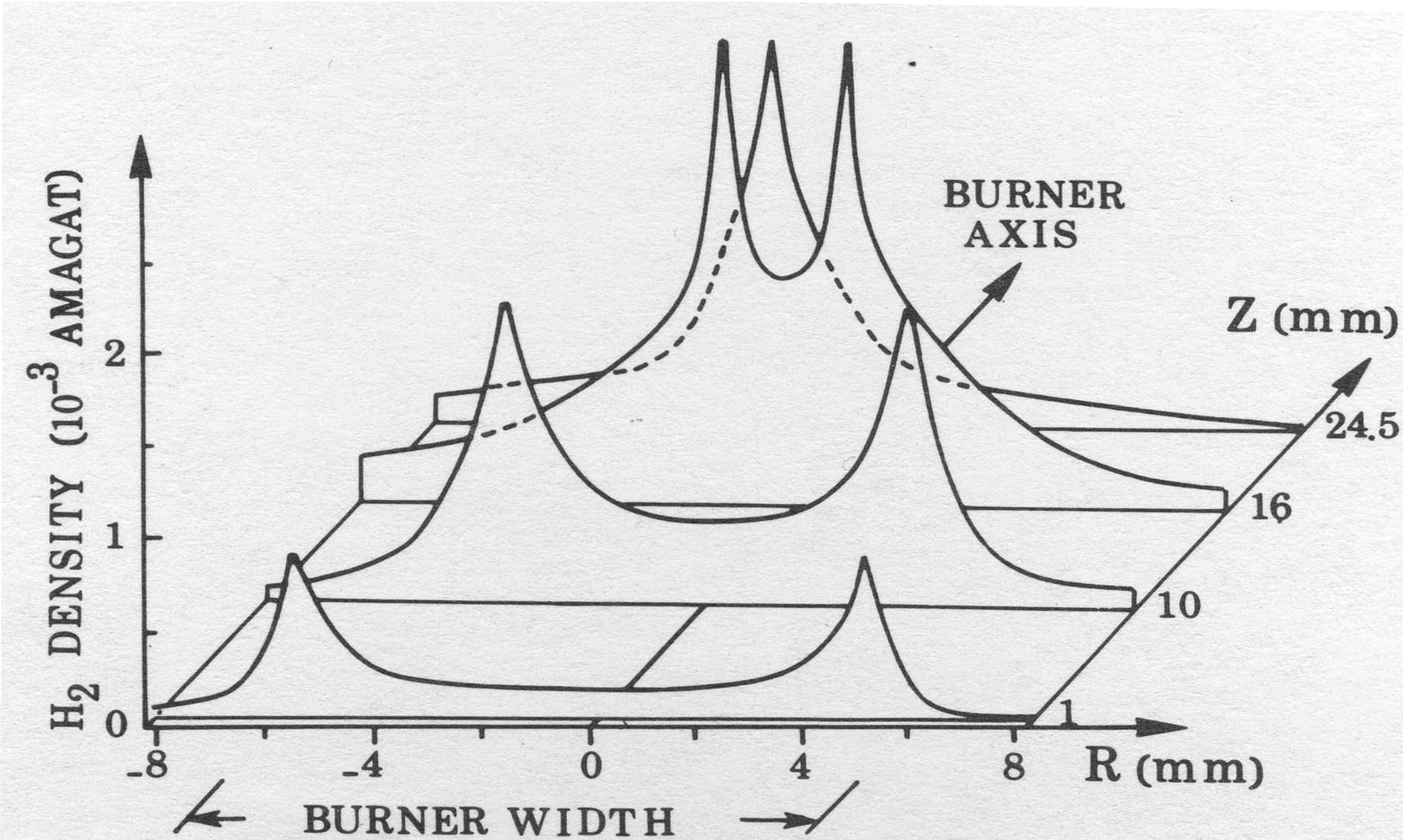

ONERA

The work in its context

- **The pioneers**
  - Maker & Terhune, Phys Rev. 137 (1965)
  - Shen & Bloembergen, Phys. Rev. 177 (1965)
  - Hauchecorne, Kerhervé & Mayer, J. Physique 32 (1971)
  - Lukasik & Ducuing, Phys Rev. Let. 28 (1972)
  - De Martini, Giuliani & Santamato, Optics Comm., 5 (1972)
  - Akhmanov & Koroteev, Sov. Phys. JETP, 40 (1974)

Making CARS a practical tool

Coherent Raman Anti-Stokes Scattering: geometry

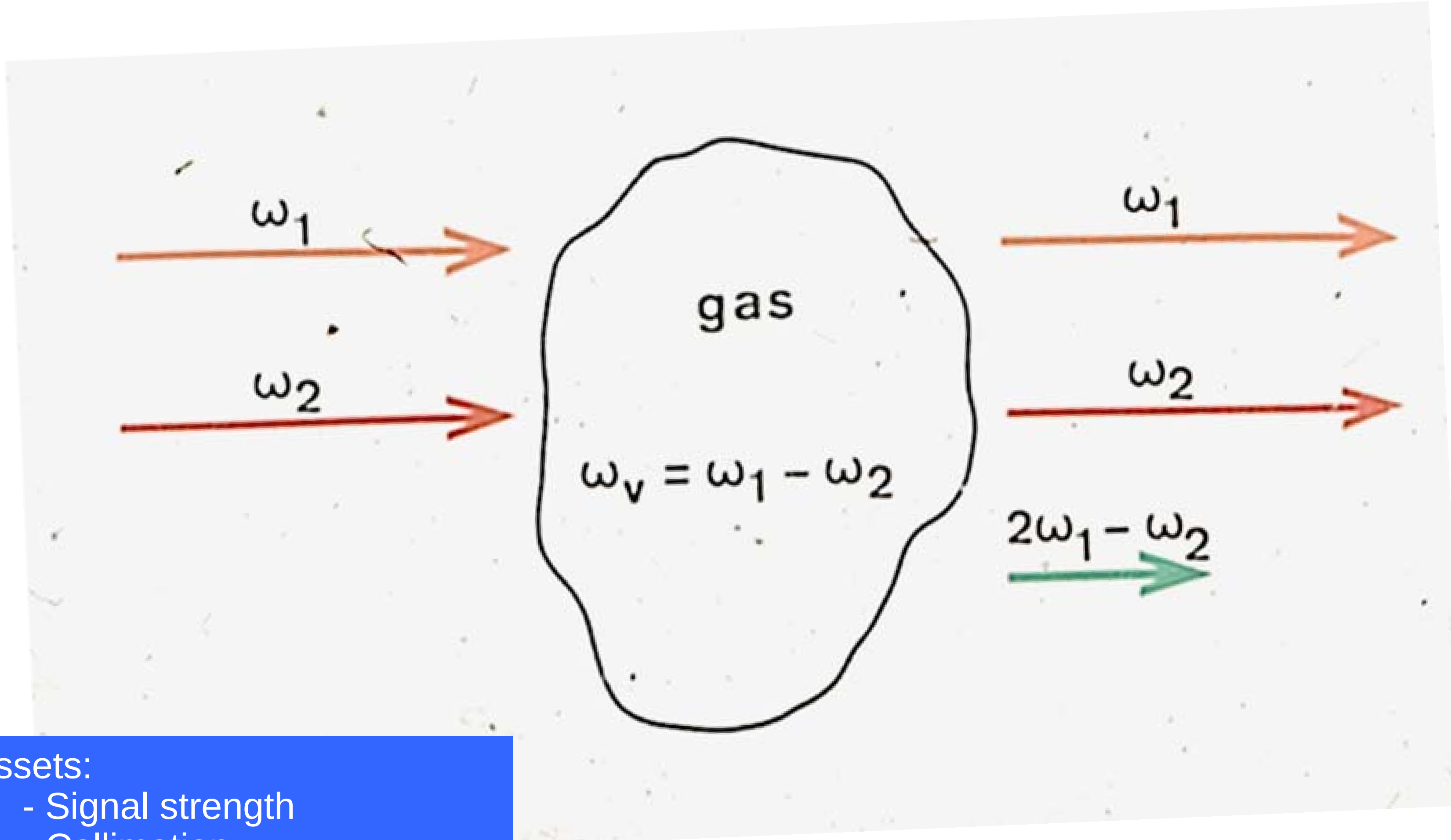

Assets:
- Signal strength
- Collimation

Spatial Resolution

- Phase-matching condition required for an efficient CARS signal production

$$\vec{k}_{CARS} = \vec{k}_3 = \vec{k}_0 + \vec{k}_1 - \vec{k}_2$$

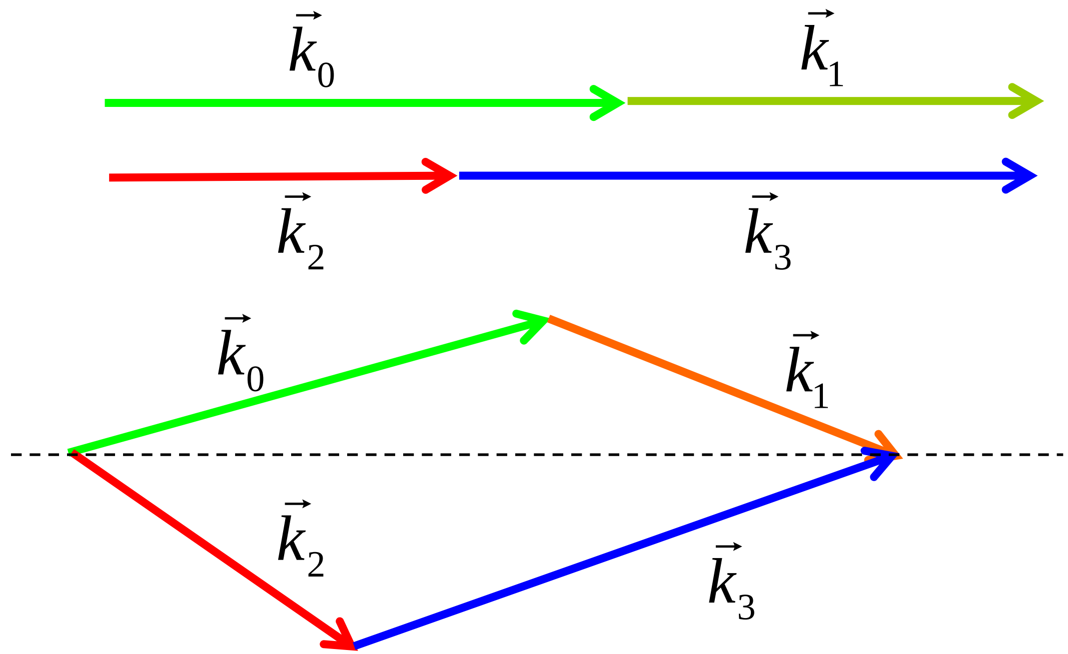

Collinear Phase-Matching

Planar Phase-Matching

Eckbreth APL (1978)

Spatial Resolution

Collinear Phase-Matching :

The confocal parameter is **4** for a **5** mm diameter beam when using a **250 mm** focal length

→ ***Poor spatial resolution***

Planar Phase-Matching :

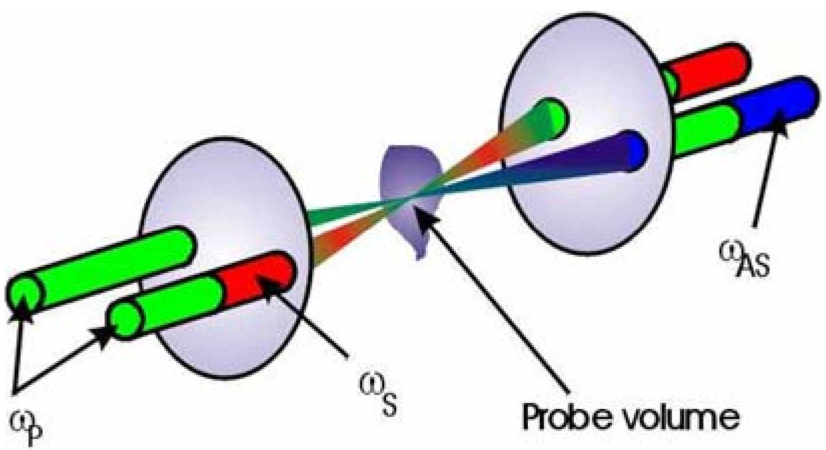

→
$$l = \frac{8\lambda f^2}{\pi \Delta d}$$

For diffraction-limited laser beams of 6 mm diameter, separated by 8.5 mm and focused with a **250 mm** focal length lens, **99 %** of the signal is created over **less than 3 mm**

Spectral analysis

Scanning CARS (only for stable media)

Laser spectral bandwidths much smaller than Raman line width.

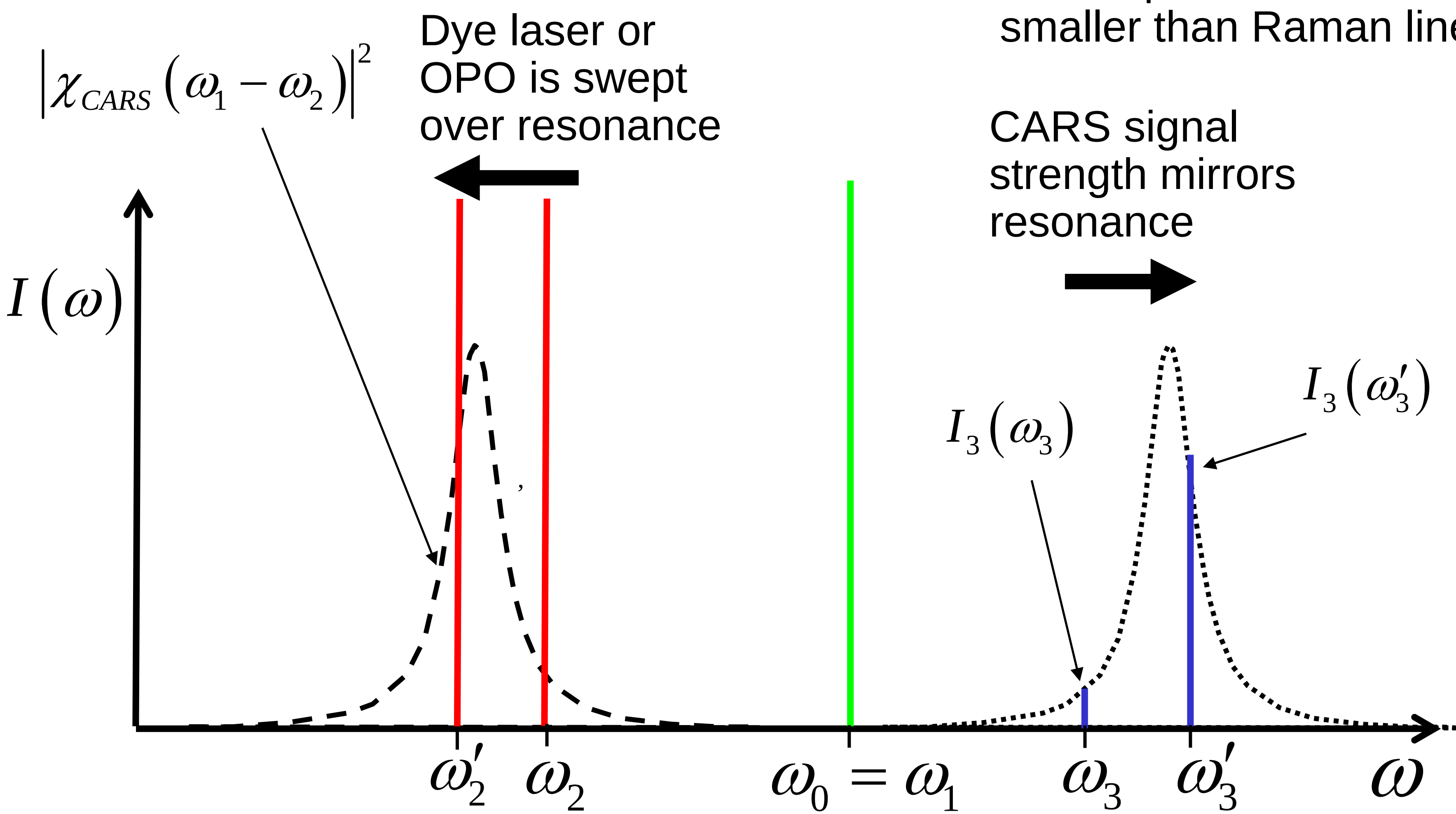

Broadband CARS (single-shot measurement for turbulent flow)

Stokes laser bandwidth larger than Raman line width, covering numerous Raman transitions.

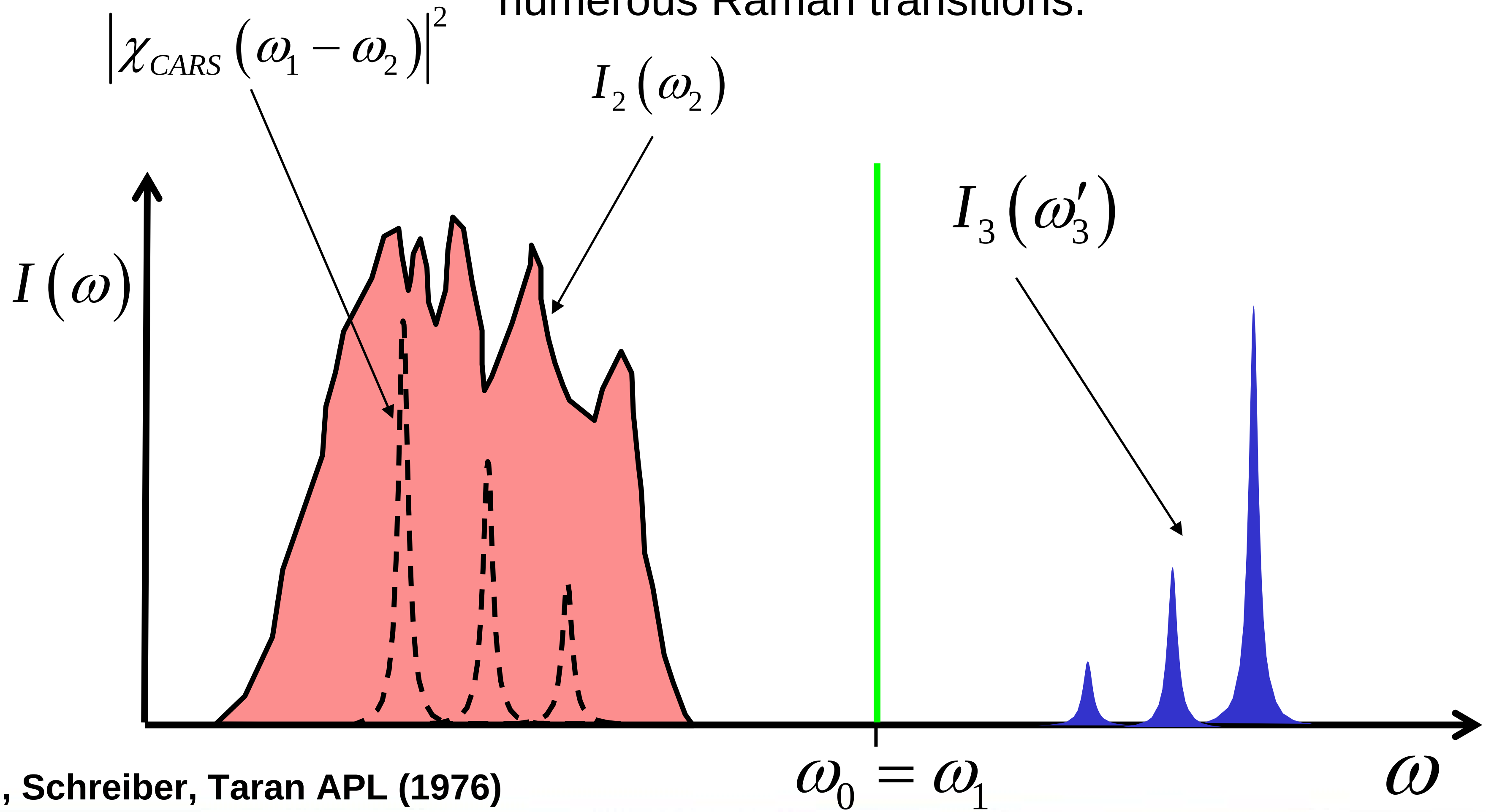

Roh, Schreiber, Taran APL (1976)

Motivation

- Improvement of the design and the optimization of high performance combustion efficiency of rocket and aircraft propulsion combustors.

- Detailed investigation of elementary processes (fuel injection, atomization, droplet vaporization, turbulent mixing, combustion,…) required.

➔ **Advanced Laser Diagnostics**

- Gaseous Combustion

- Two-phase Combustion

Liquid : *Kerosene/Air Combustion*

LOX/GH$_2$,LOX/CH$_4$ Cryogenic Combustion

Solid : *Solid Propellant Combustion*

- Non-reactive flows

Turbulence , mixing layer, ...

Vulcain 2

CFM 56

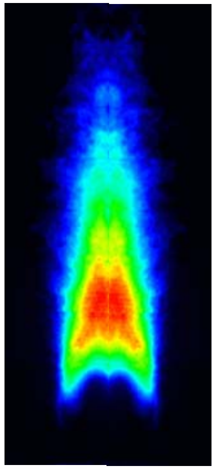

ONERA

CARS Diagnostic (temperature and species concentration)

- CARS signal several orders of magnitude stronger than spontaneous Raman scattering.
- CARS produces a coherent signal beam that can be fully collected whereas a small fraction of the scattered light is collected for incoherent processes.
- Thermal background radiation can be eliminated because the CARS beam is collected within a small solid angle.
- Signal, shifted to shorter wavelengths than those of the laser beams, has little interference from laser-induced fluorescence.
- Using a broadband single-shot procedure, single-shot measurements are possible with good spatial resolution and good detectivity ~ 10^{17} mol/cm^3.

CARS process: theory

➢ **Four wave mixing process**

Step 1 : Coherent Excitation of the vibrational state in the fundamental electronic states.

Use two laser waves with a wavelength difference equal to the vibrational frequency of the probed molecule.

Step 2 : Probe the coherent excitation *via* a third laser beam (usually, $\omega_0 = \omega_1$) .

Step 3 : Produce an anti-Stokes beam characteristic of the thermodynamic properties of the molecule

$$\omega_{CARS} = \omega_3 = \omega_0 + \omega_1 - \omega_2$$

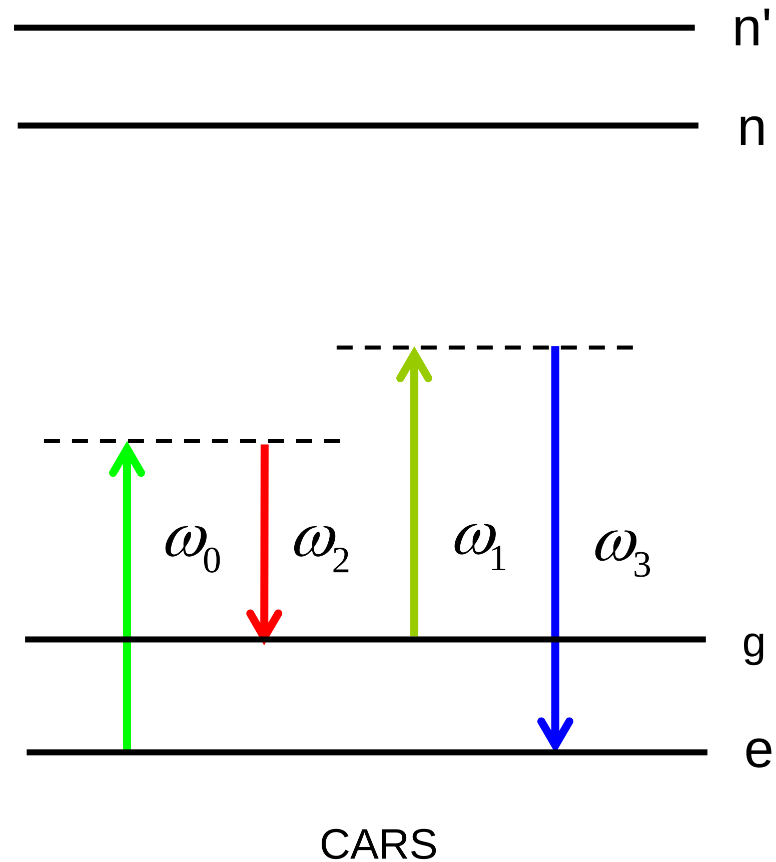

Energy level diagram

Fundamental aspects of CARS

The wave equation which governs the propagation of optical wave *E*(**r**) in a medium is

$$\nabla^2 \vec{E}\left(\omega_j,\vec{r}\right) + \frac{\omega_j^2}{c^2}\vec{E}\left(\omega_j,\vec{r}\right) = -\mu_0\,\omega_j^2\,\vec{P}\left(\omega_j,\vec{r}\right)$$

In an isotropic medium, the polarization at ω_3 is given by

$$\vec{P}\left(\omega_3,\vec{r}\right) = \vec{P}^{(1)}\left(\omega_3,\vec{r}\right) + \vec{P}^{(3)}\left(\omega_3,\vec{r}\right) = \varepsilon_0\,\chi^{(1)}\,\vec{E}\left(\omega_3,\vec{r}\right) + \vec{P}^{(3)}\left(\omega_3,\vec{r}\right)$$

(Summation of linear and nonlinear terms)

This expression can also expressed as

$$P_i^{(3)}\left(\omega_3,\vec{r}\right) = \varepsilon_0\,\chi_{ijk\ell}^{(3)}\left(-\omega_3,\omega_0,\omega_1,\omega_2\right)E_j\left(\omega_0,\vec{r}\right)E_k\left(\omega_1,\vec{r}\right)E_\ell\left(\omega_2,\vec{r}\right)$$

$$\omega_0 + \omega_1 + \omega_2 - \omega_3 = 0$$

The Third-Order Susceptibility

$$P_x^{(3)}(\omega_3,\vec{r}) = \varepsilon_0\, 3\, \chi_{xxxx}^{(3)}(-\omega_3, \omega_1, \omega_1, -\omega_2)\, E_x^2(\omega_1,\vec{r})\, E_x(-\omega_2,\vec{r})$$

$$P^{(3)}(\omega_3,\vec{r}) = \varepsilon_0\, \chi_{CARS}\, E^2(\omega_1,\vec{r})\, E(-\omega_2,\vec{r})$$

The wave equation for a CARS signal beam propagating along the z-axis is given by

$$ik_3 \frac{\partial E(\omega_3)}{\partial z} \exp(i\, k_3\, z) = -\frac{\omega_3^2}{c^2} \chi_{CARS}\, E^2(\omega_1)\, E^*(\omega_2) \exp\left[i\left(2\vec{k}_1 - \vec{k}_2\right)\bullet \vec{r}\right]$$

The Wave Equation and the Third-Order Susceptibility

When the phase-matching condition is satisfied then

$$\exp\left(i\,k_3\,z\right) \;=\; \exp\left[i\left(2\vec{k}_1 - \vec{k}_2\right)\bullet\vec{r}\,\right]$$

and

$$E\left(\omega_3\right) \;=\; i\,k_3\,\frac{\omega_3^2}{c^2}\,\chi_{CARS}\;E^2\left(\omega_1\right)E^*\left(\omega_2\right)\int_0^{\ell} dz$$

$$=\; i\,\frac{\omega_3}{c}\,\chi_{CARS}\;E^2\left(\omega_1\right)E^*\left(\omega_2\right)\,\ell$$

The intensity of the CARS signal is then given by

$$I_3 \;=\; \frac{1}{2}c\,\varepsilon_0\left|E\left(\omega_3\right)\right|^2 \;=\; \frac{\omega_3^2}{c^4\,\varepsilon_0^2}\,I_1^2\,I_2\left|\chi_{CARS}\right|^2\,\ell^2$$

ONERA

CARS Susceptibility

$$I_{CARS} = I_3 \propto \left|\chi_{CARS}(\omega_1, \omega_2)\right|^2 I_1^2\, I_2\, \ell^2$$

$$\chi^{(3)}(\omega) = \chi_R^{(3)}(\omega) + \chi_{NR}^{(3)}(\omega)$$

Resonant term   Non-resonant term

$$\chi_R^{(3)}(\omega) = \frac{iN}{\hbar}\sum_j \alpha_j \sum_k \alpha_k \Delta\rho_k^{(0)} G_{jk}^{-1}$$

$$G_{jk} = i(\omega_P - \omega_S - \omega_R)\delta_{jk} + (\frac{\Gamma_j}{2} - i\Delta_j)\delta_{jk} + W_{jk}(1-\delta_{jk})$$

χ_{nr} depends on the effects of remote vibrational resonances and those associated with the nonlinear distortion of the electron cloud of the molecules caused by the intense laser fields)

Polarization Arrangement

Goal: Cancelling the non-resonant contribution

$$\vec{E}(\omega_3) = 3i\frac{\omega_3}{2c}\left[\chi^{(3)}_{1122}\,\hat{e}_0(\hat{e}_1\bullet\hat{e}_2) + \chi^{(3)}_{1212}\,\hat{e}_1(\hat{e}_0\bullet\hat{e}_2) + \chi^{(3)}_{1221}\,\hat{e}_2(\hat{e}_0\bullet\hat{e}_1)\right] \times E(\omega_0)E(\omega_1)E^*(\omega_2)\,\ell$$

•The two pump beams are propagating separately and with different polarizations, the angles between the x axis and the incident field polarizations are θ_i.

• Analysing of the two fields using a polarizer rotated by angle Φ with respect to the x axis.

$$P_3 = 1.3\times10^{-46}\,\omega_3^{\,4}P_1P_1^{'}P_2\left|\begin{array}{l}\chi^{(3)}_{1111R}\cos\theta_1^{'}\cos\theta_1\cos\Phi + \chi^{(3)}_{1221R}\sin\theta_1^{'}\sin\theta_1\cos\Phi + \chi^{(3)}_{1122R}\sin(\theta_1^{'}+\theta_1)\sin\Phi \\ +\chi^{(3)}_{1111NR}(\cos\theta_1^{'}\cos\theta_1\cos\Phi + \frac{1}{3}\sin\theta_1^{'}\sin\theta_1\cos\Phi + \frac{1}{3}\sin(\theta_1^{'}+\theta_1))\sin\Phi\end{array}\right|^2$$

Complete rejection of the non resonant contribution

But reduction of the signal by a factor of 16

$$\theta_1^{'} = \theta_1 = 120^\circ$$

$$\Phi = 60^\circ$$

Experimental Setup

Pump Laser: seeded Nd:YAG laser operating in the green.

Stokes laser: Broadband dye laser or OPO

Reference channel: flow of Argon

Nonresonant CARS signal created to monitor the shot to shot fluctuations of direction and of pulse energy of the lasers beams and of the spectral shape of the Stokes laser.

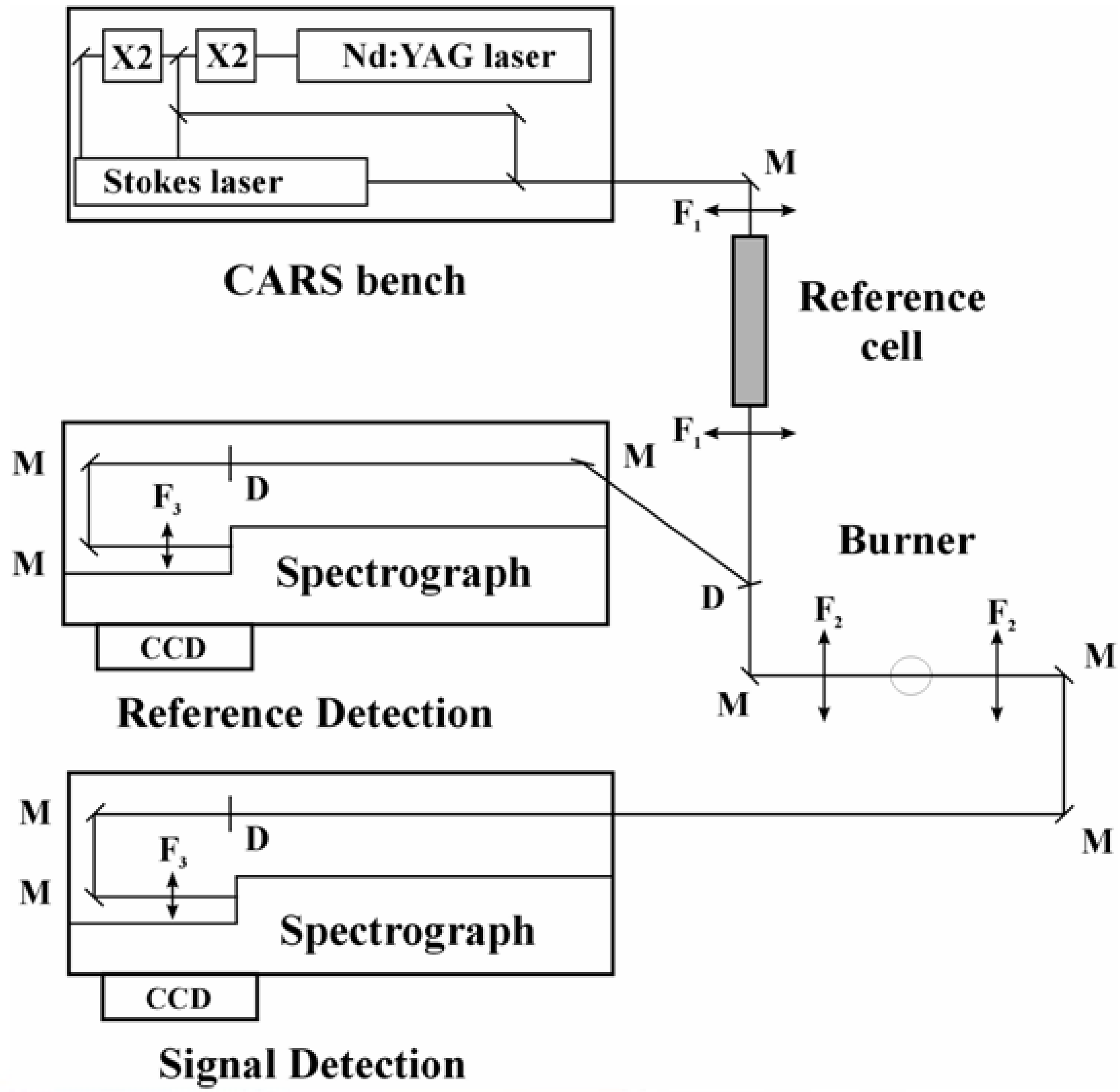

Coherent Anti-Stokes Raman Scattering Measurements of Temperature and Concentration

CARS Temperature Measurements

Nitrogen CARS is widely used for temperature measurements in flames, sophisticated models of the nitrogen CARS spectrum have been developed.

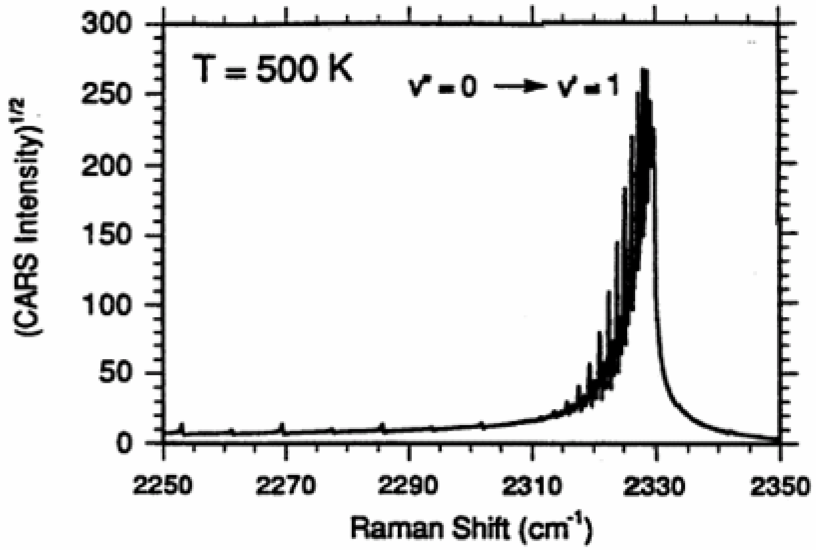

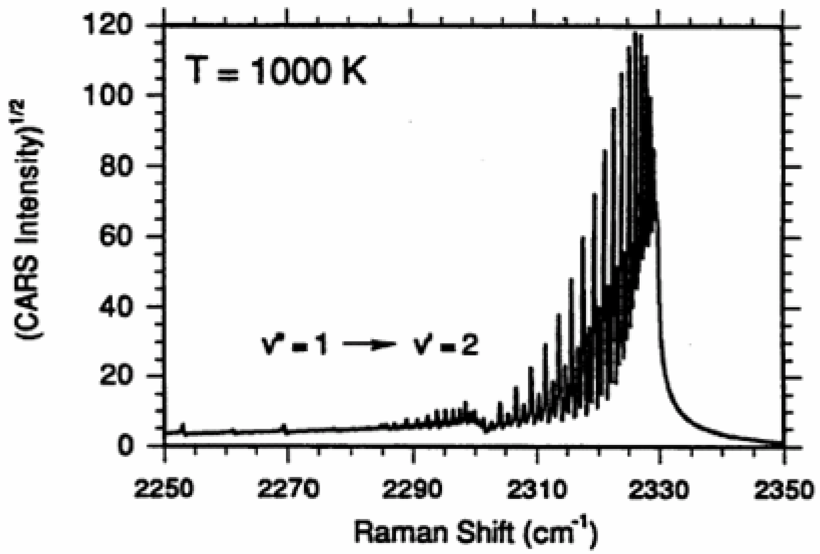

ONERA

CARS Temperature Measurements

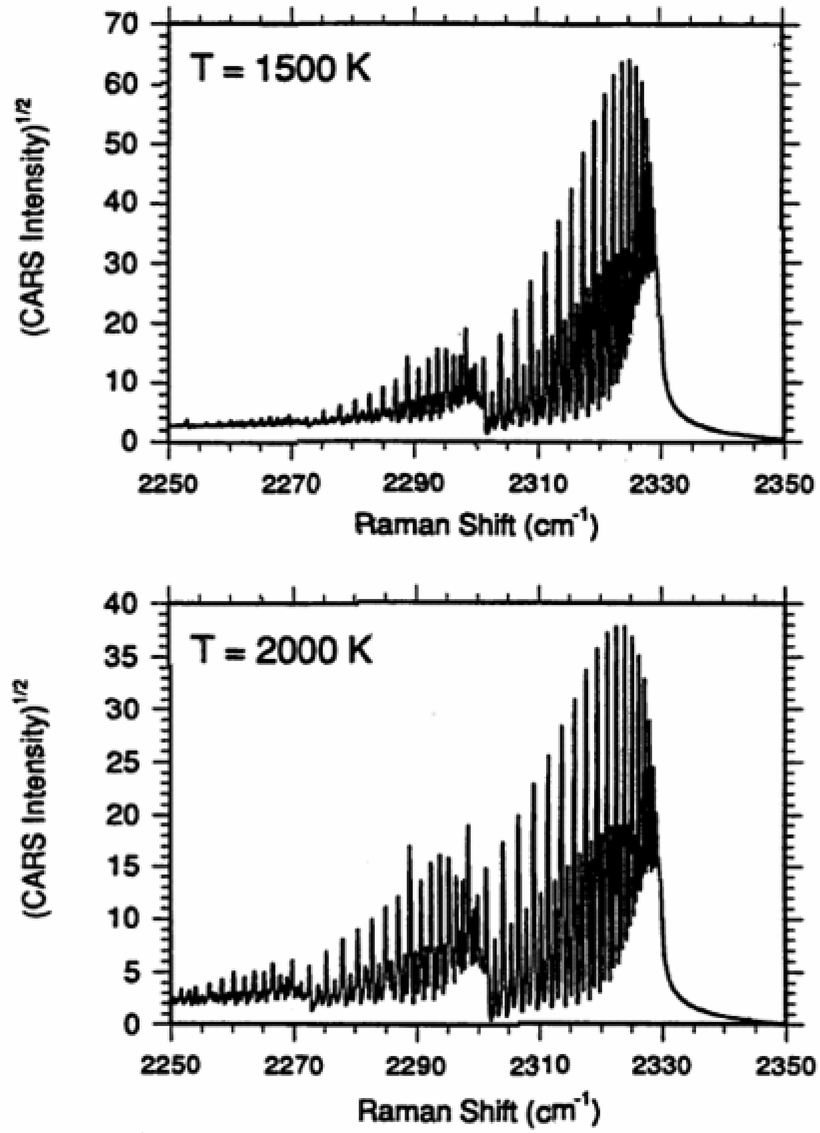

CARS Temperature Measurements

Raman linewidths $\Gamma_j = 2\gamma_j$ are needed for modeling of the N_2 CARS spectrum.

L. Rahn and R. Farrow

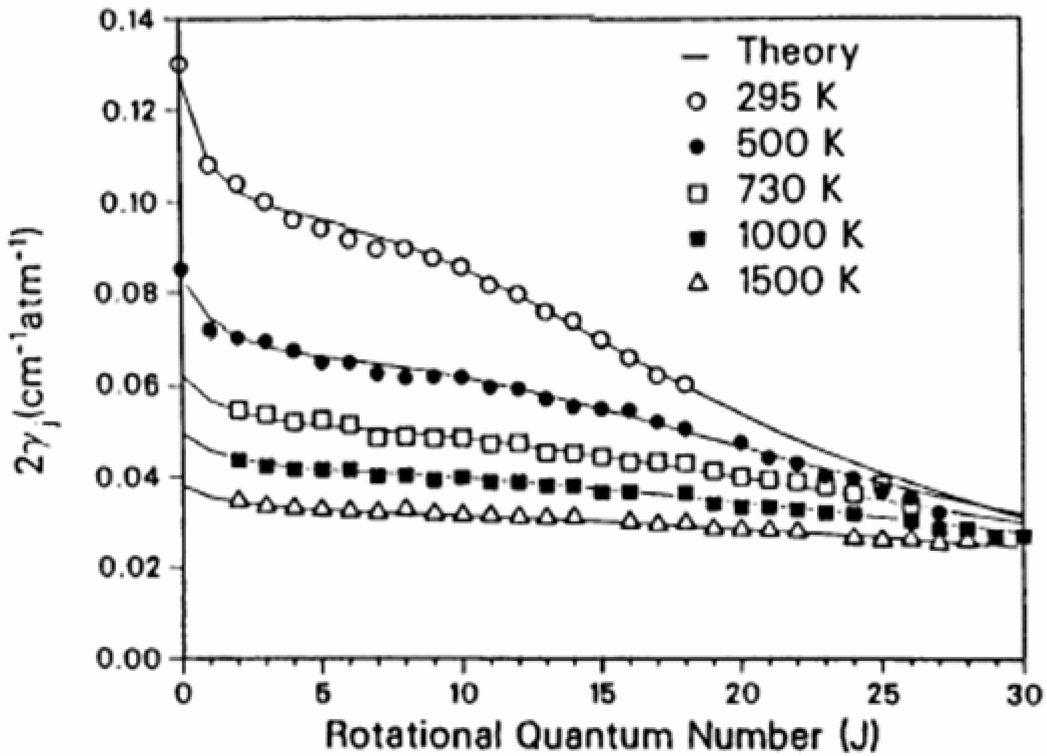

FIG. 7. N_2-N_2 collisional self-broadening coefficients as a function of temperature and rotational quantum number J. The symbols represent experimental values determined by Galatry model fits to each line, including overlap from the wings of neighboring lines. The solid curves are predictions from the modified exponential energy-gap (MEG) scaling law discussed in the text.

Collisional Narrowing of the CARS Spectrum

Collisional narrowing causes a collapse of the nitrogen Q-branch spectrum at high pressures. Effect must be modeled accurately because a pressure increase and a temperature decrease have approximately the same effect on the spectrum.

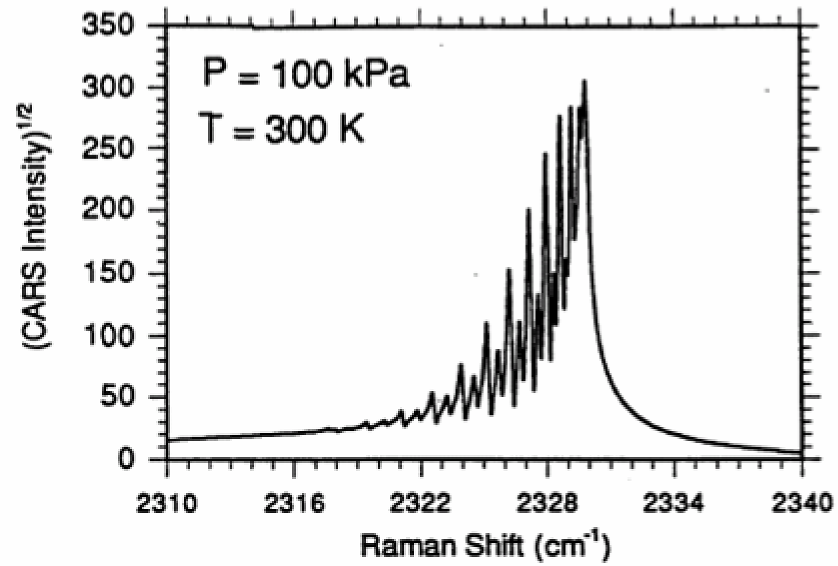

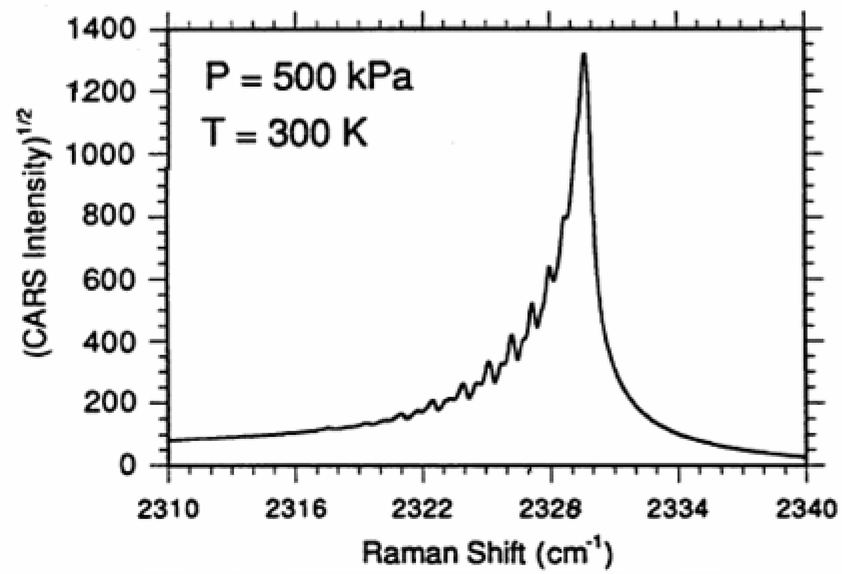

Collisional Narrowing of the CARS Spectrum

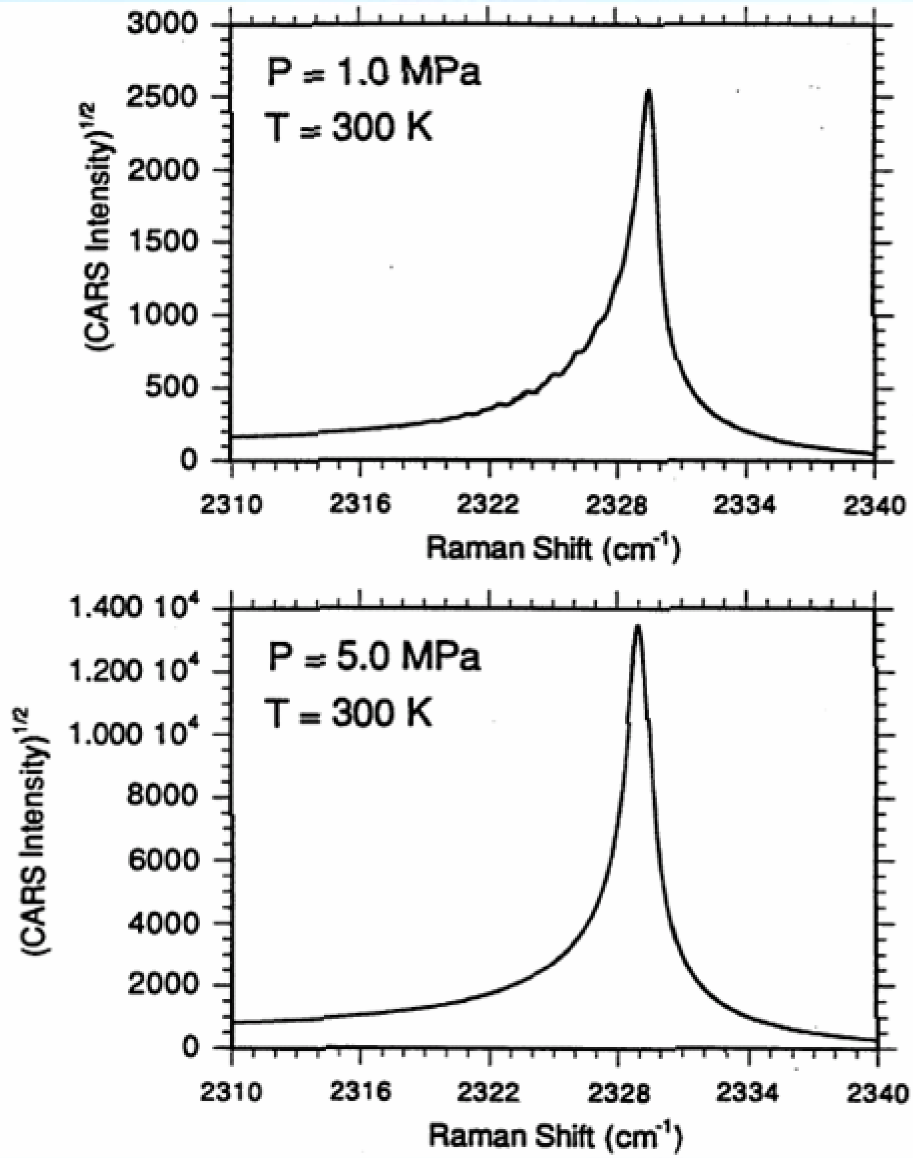

Data Processing

Data processing is performed by comparing the experimental spectra to the theoretical ones using a least-square fitting routine.

$$(\log I_{\mathrm{i}}^{\exp} - \log I_{i}^{theo}) I_{i}^{theo}$$

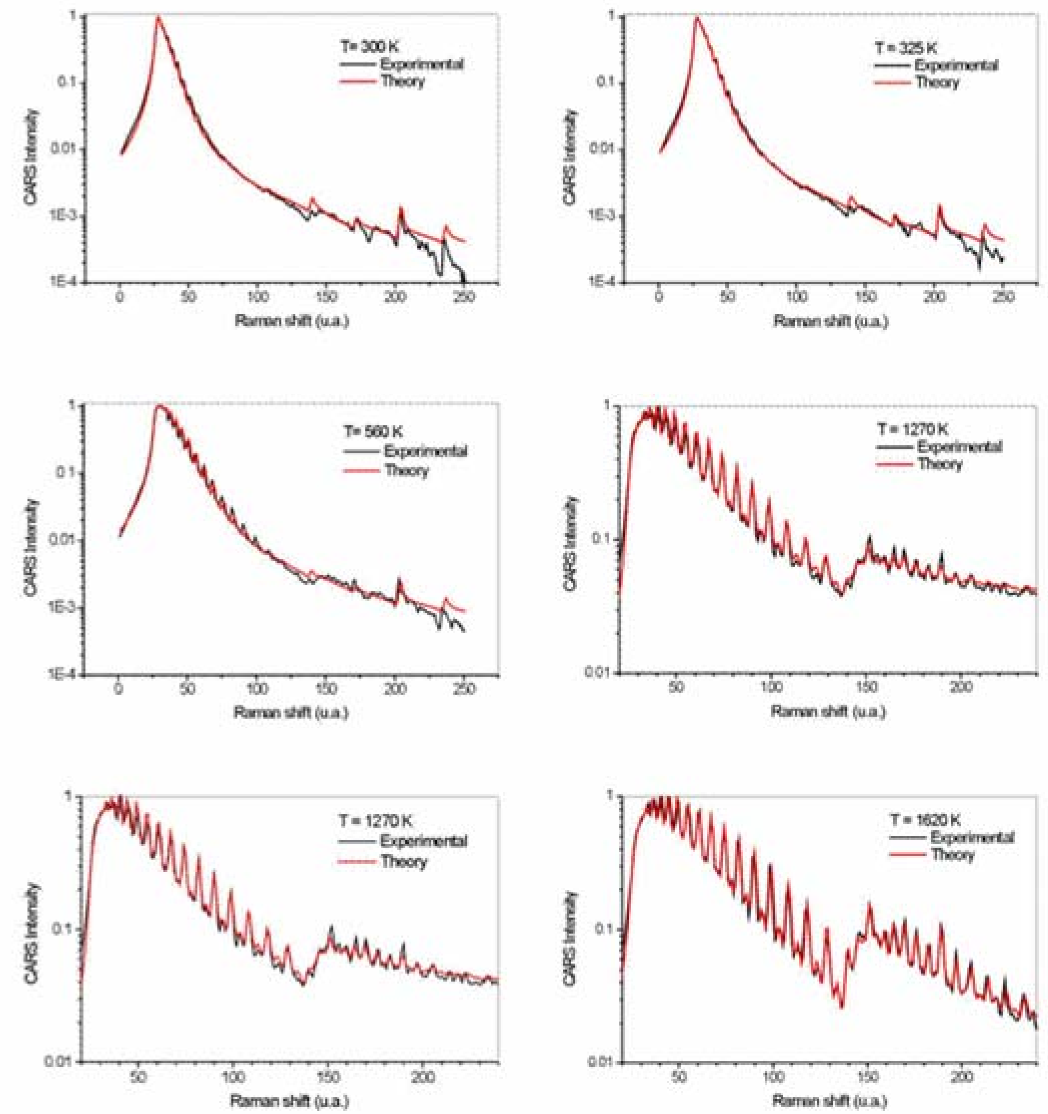

Applications

Buoyant diffusion H_2/air flame

- Cooperation with M. Roquemore and V. Katta (Wright Patterson Air Force Base, Dayton, USA)

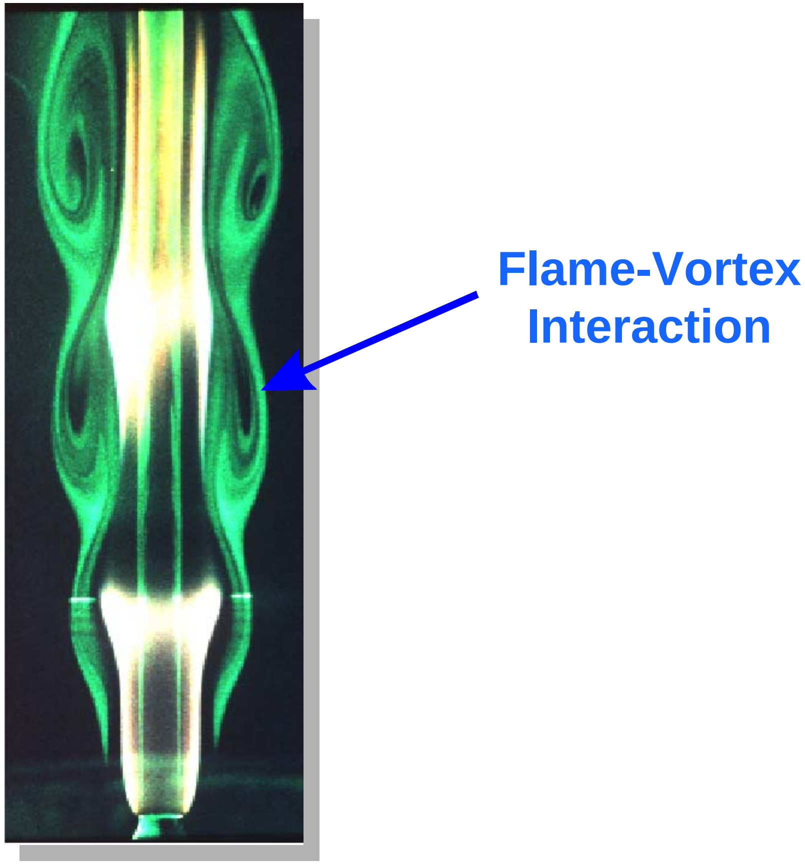

H_2/air Flame

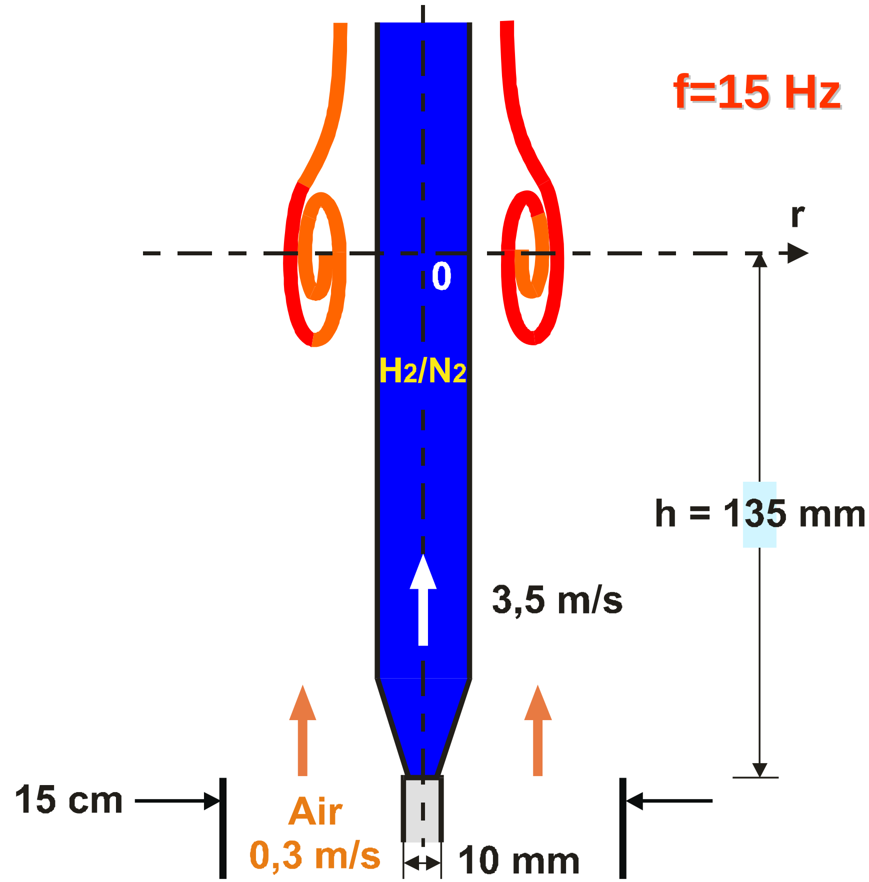

- Large domain of temperature and species concentration investigated

N_2 - CARS Thermometry

Data processing

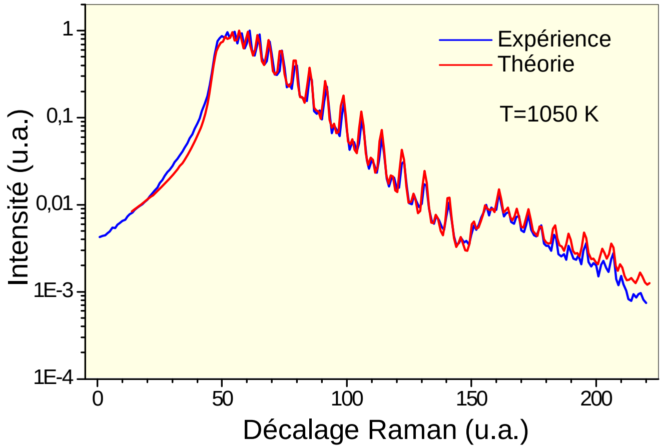

Temporal profile

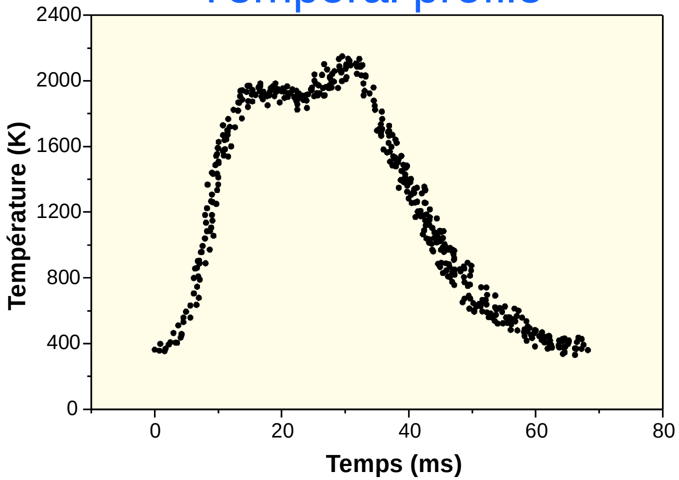

r= 15.5 mm

Temperature

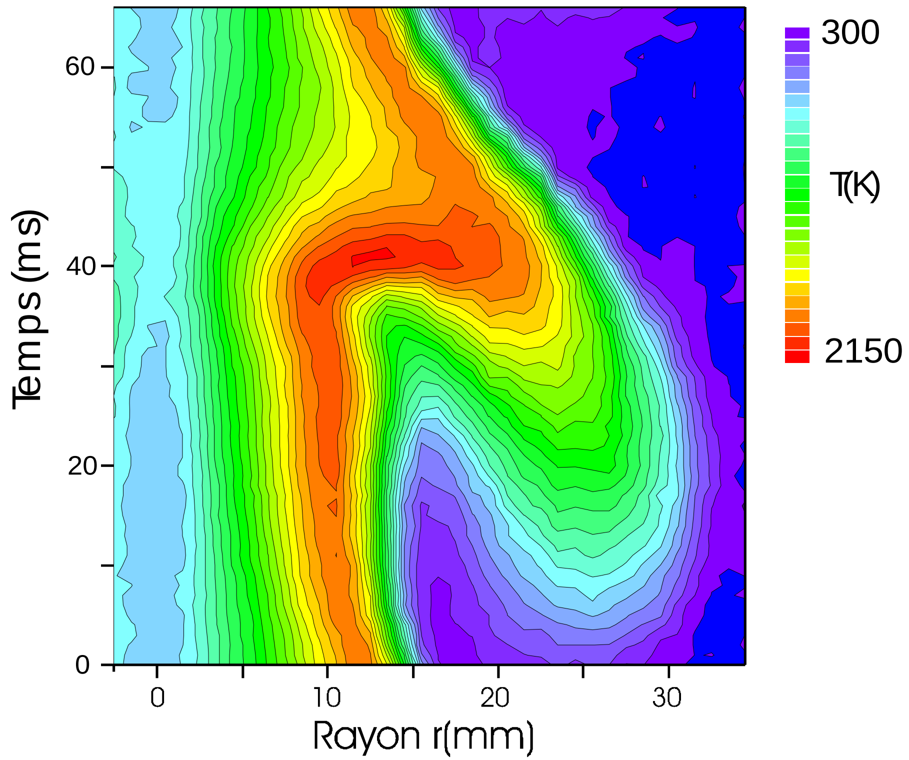

Temperature accuracy : 2 %

H_2 - CARS Thermometry and Concentration

Data processing

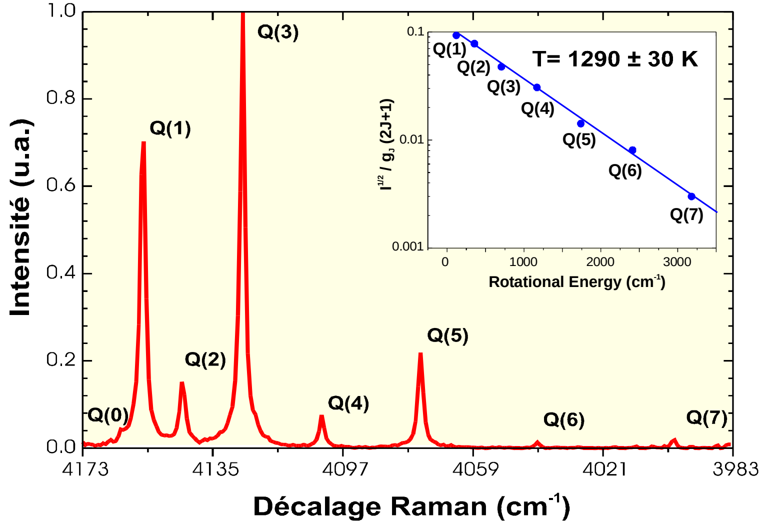

Temporal profile

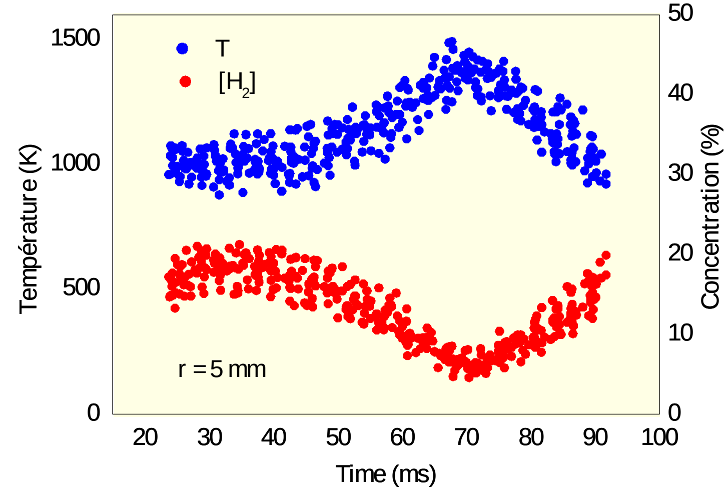

Calibration procedure

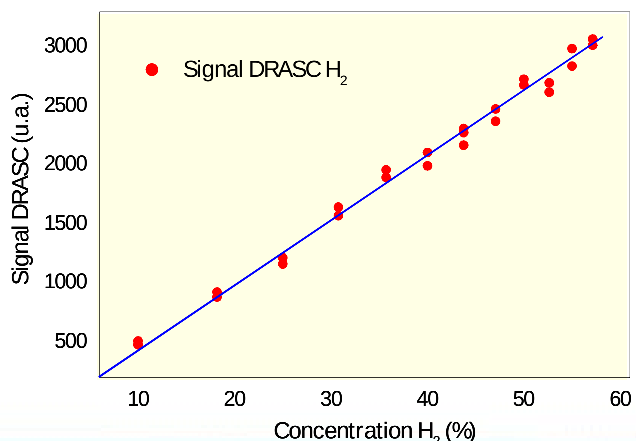

Laminar H_2-Air

At room temperature

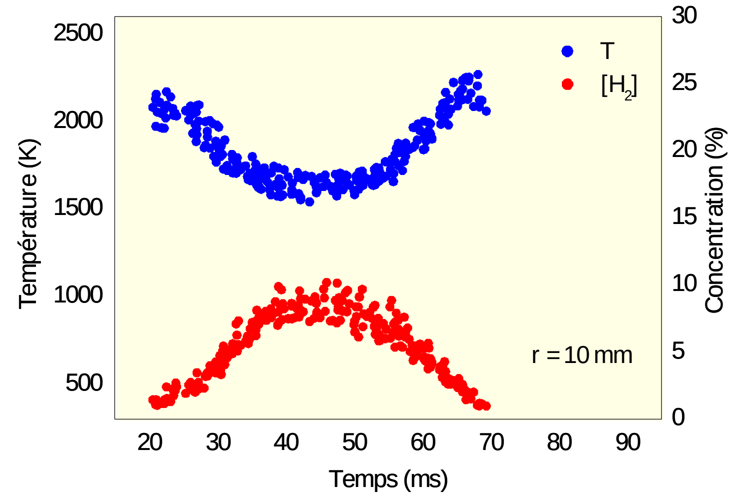

H_2 - CARS Thermometry and concentration

Comparison Temperature N_2 - H_2

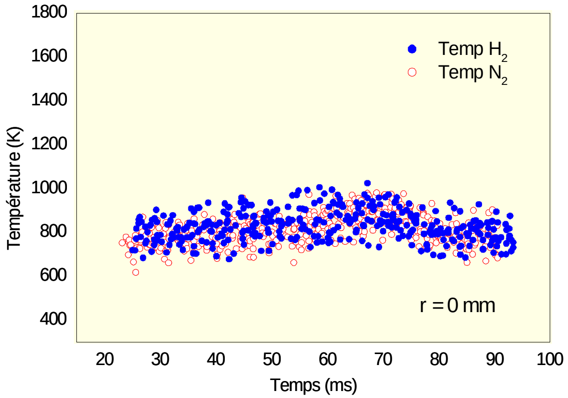

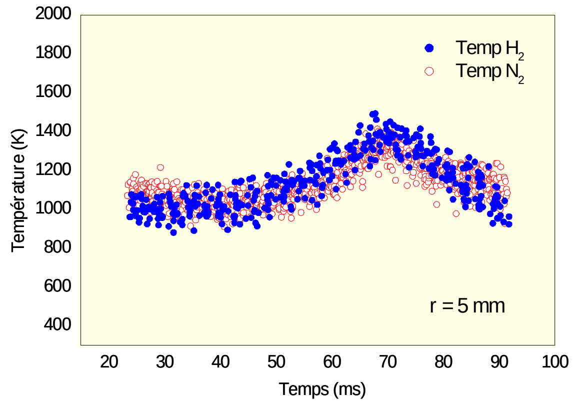

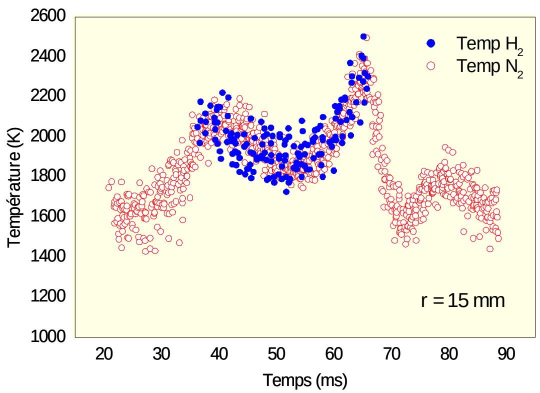

H_2 Concentration

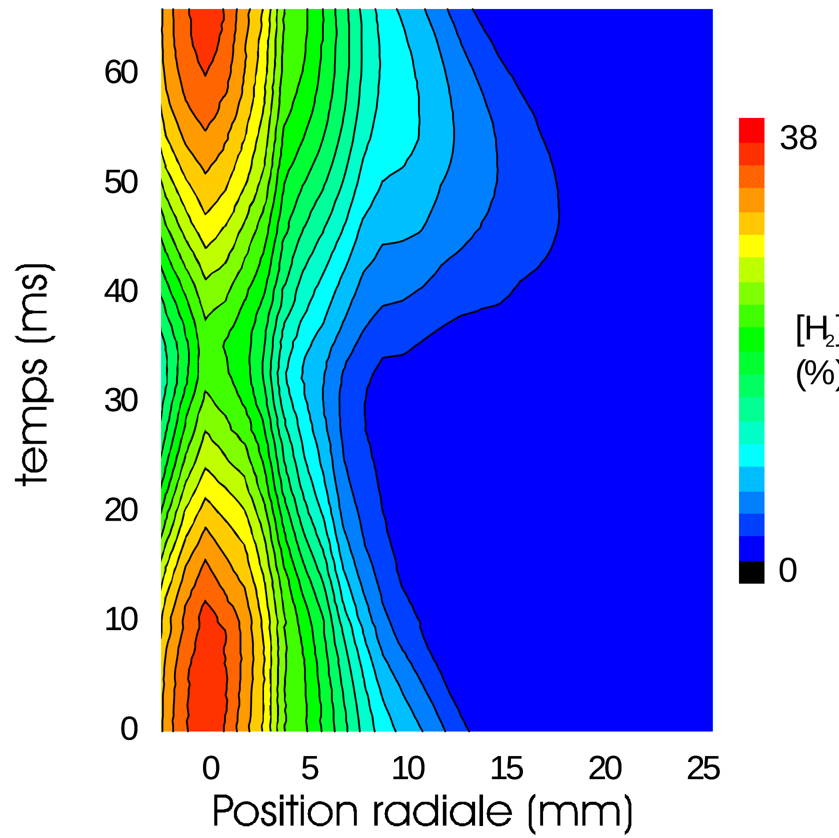

Temperature accuracy ≈ 2 %

Comparison between Experiment and Theory

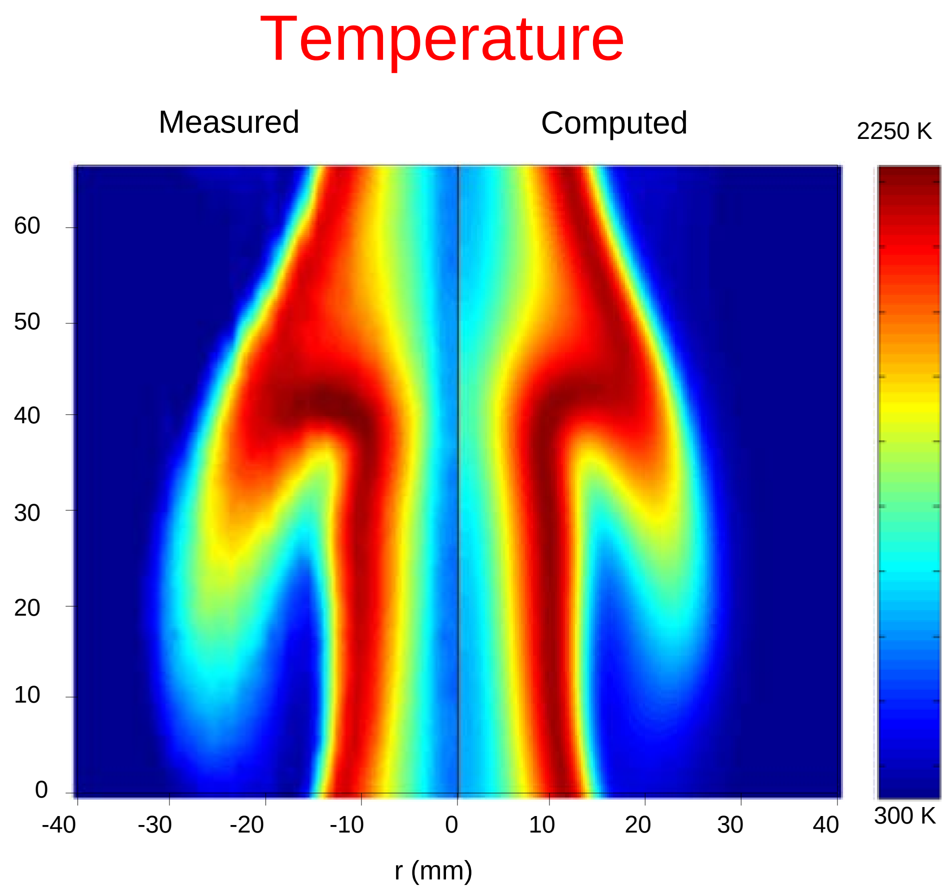

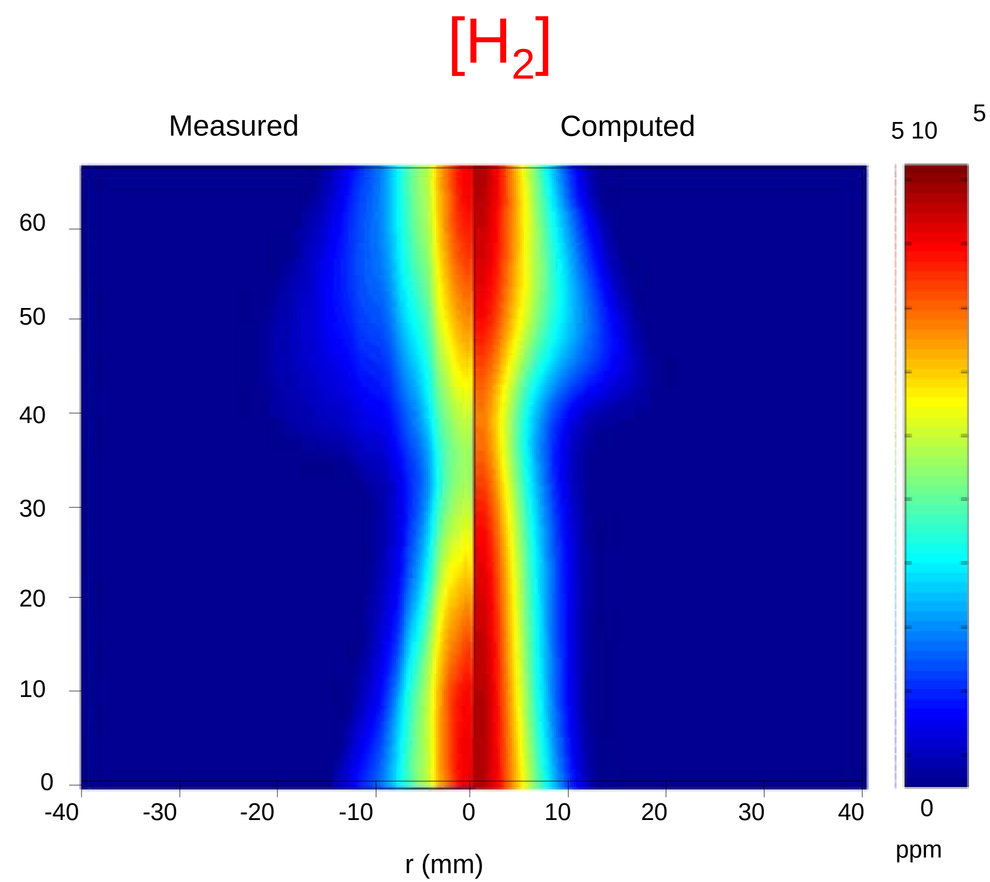

Simulation performed by V. Katta & M. Roquemore (Wright-Patterson Air Force Base, Dayton, USA)

Cryogenic Propellant Combustion

- Investigation focused on Liquid Oxygen and gaseous Hydrogen reactants
- Propellant used in many performance engines like Vulcain (Ariane 5)

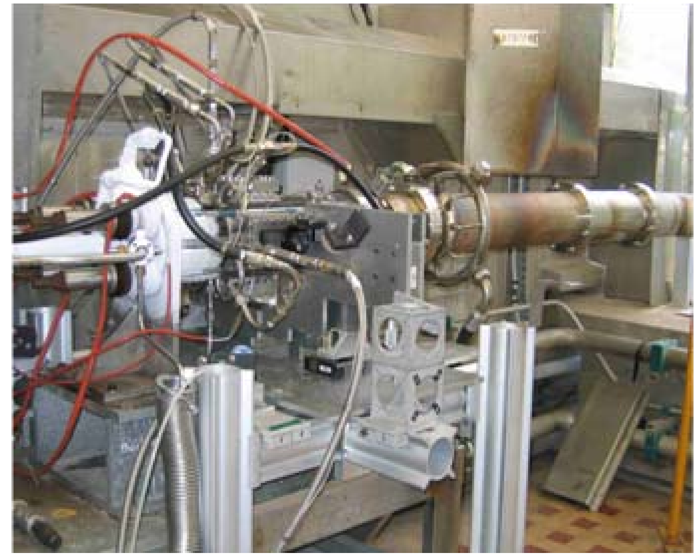

Mascotte facility (Onera)

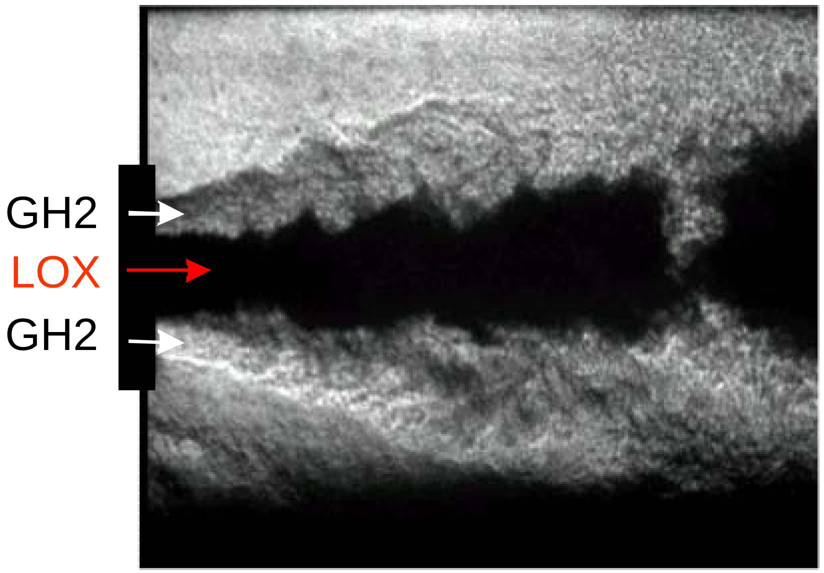

Flame Vizualisation at 3.0 MPa using Shadowgraph

➔ ***Temperature and Species concentration measurements***

➡ ***Probing of H_2 and H_2O***

Cooperation with DLR and GPI

Experimental Setup

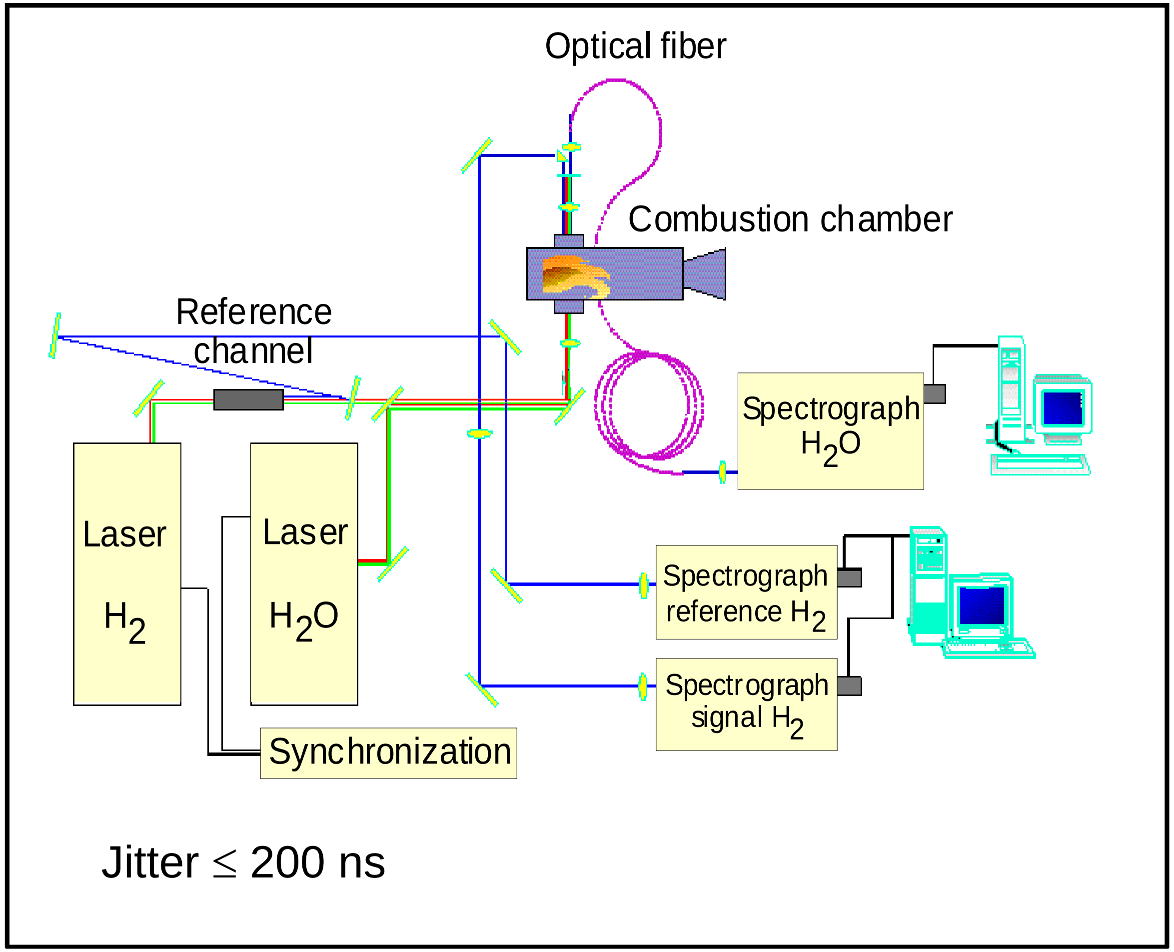

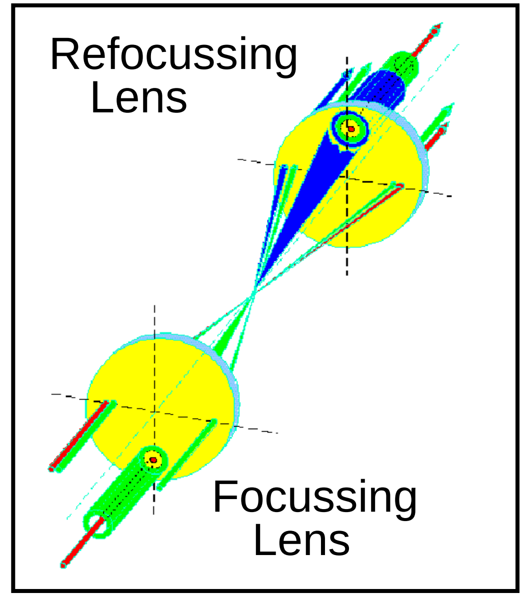

- Laser beam arrangement:

  H_2 : Planar BOXCARS
  H_2O: USED CARS

- Probe volume dimensions:

  H_2 : 0.8 mm × 100 μm
  H_2O: 2 mm × 150 μm

High Pressure H_2 CARS Spectra

- Single-shot measurements

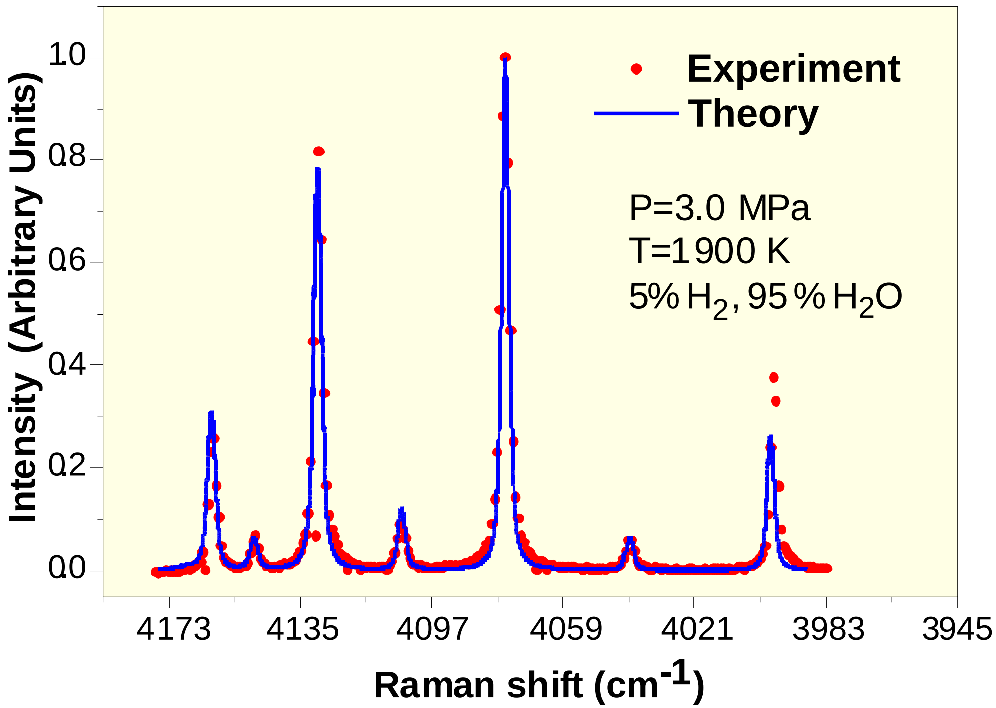

Subcritical (for O) Pressure

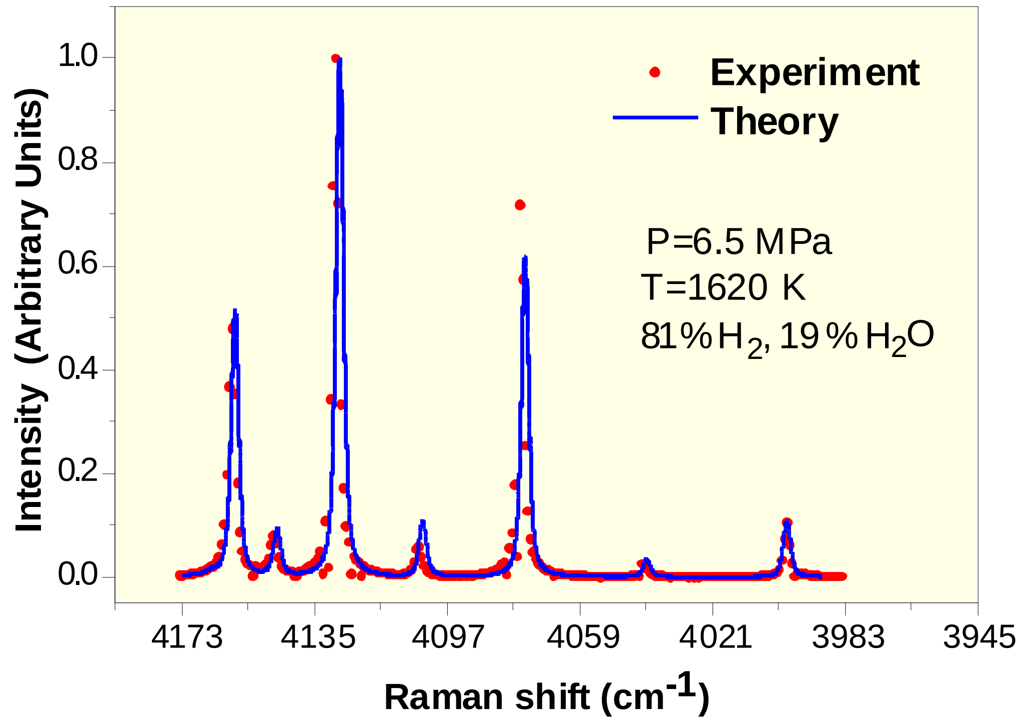

Supercritical Pressure

Cryogenic Combustion at 3.0 MPa

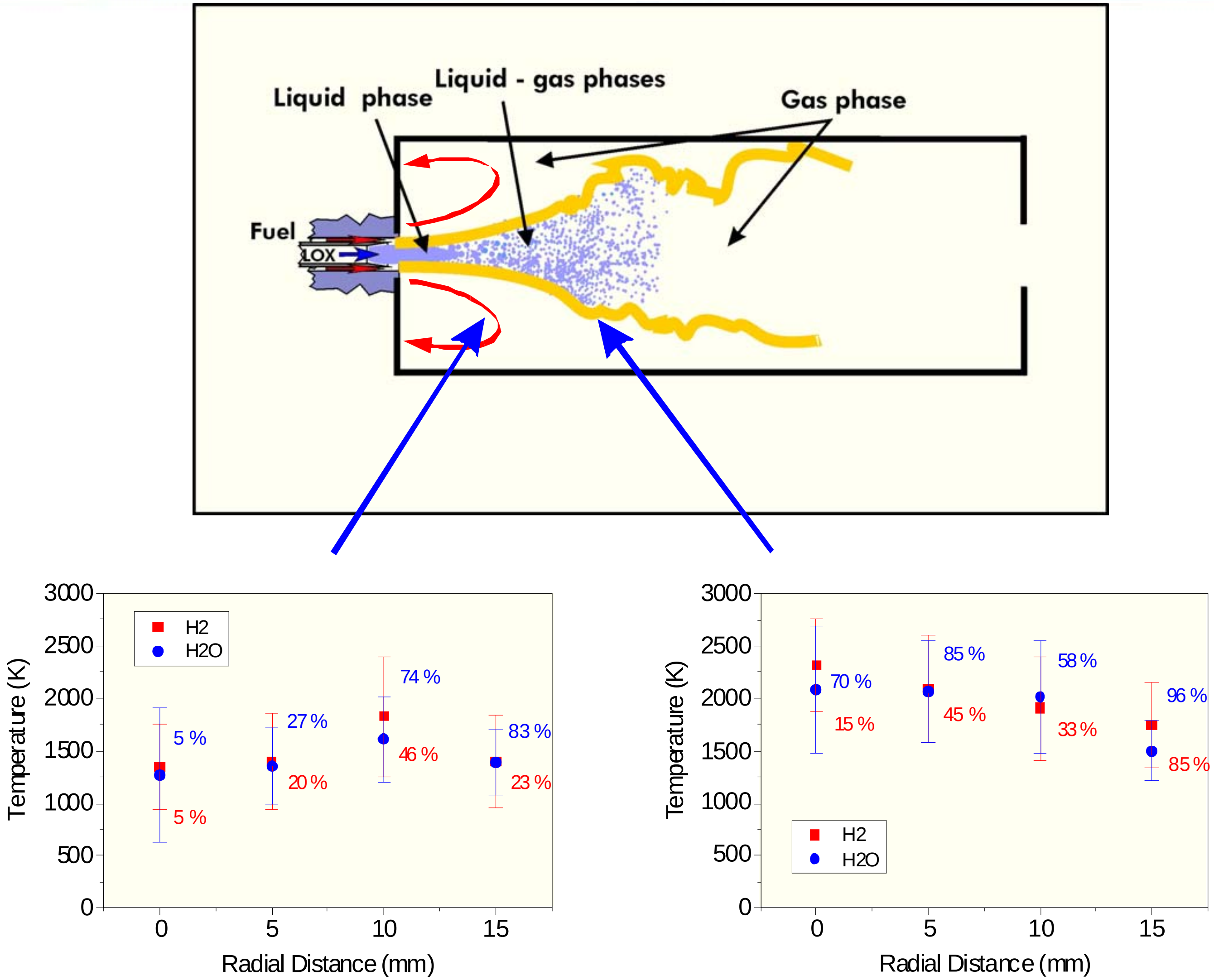

X = 50 mm **X = 100 mm**

$$\dot{m}_{H_2} = 25\,\mathrm{g/s}$$

$$\dot{m}_{H_2O} = 50\,\mathrm{g/s}$$

Temperature Probability Density Function

Supercritical Condition (P=6.5 MPa)

- Series of 300 single-shot measurements with a validation rate exceeding 80 %

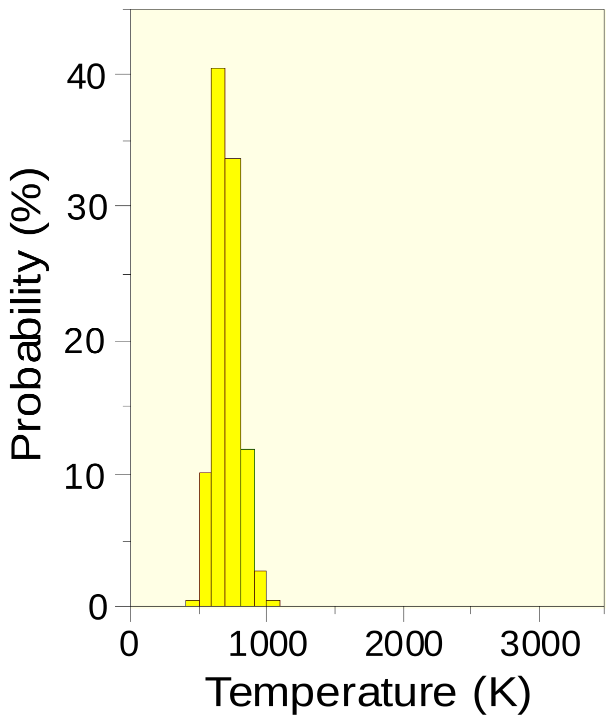

X = 15 mm, Y=15 mm

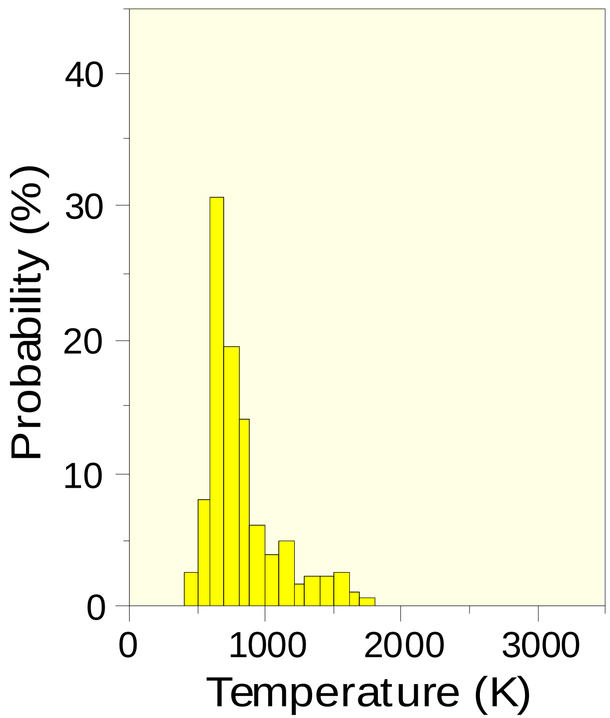

X = 50 mm, Y=15 mm

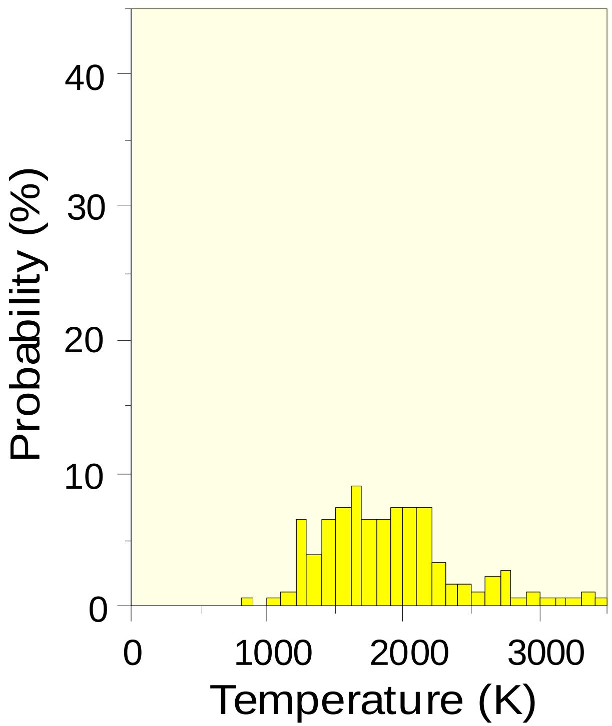

X = 150 mm, Y=15 mm

$$\dot{m}_{H_2} = 45\,\text{g/s} \qquad \dot{m}_{H_2O} = 100\,\text{g/s}$$

Cryogenic Combustion LOX/CH_4

■ CARS Thermometry on CH_4

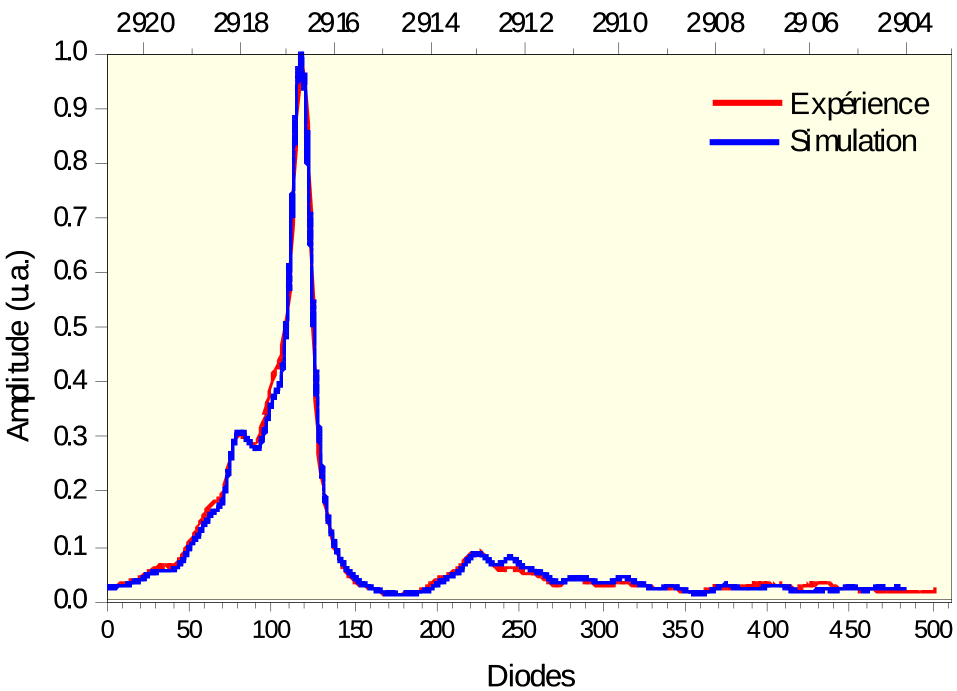

P = 0.1MPa, T= 1200 K

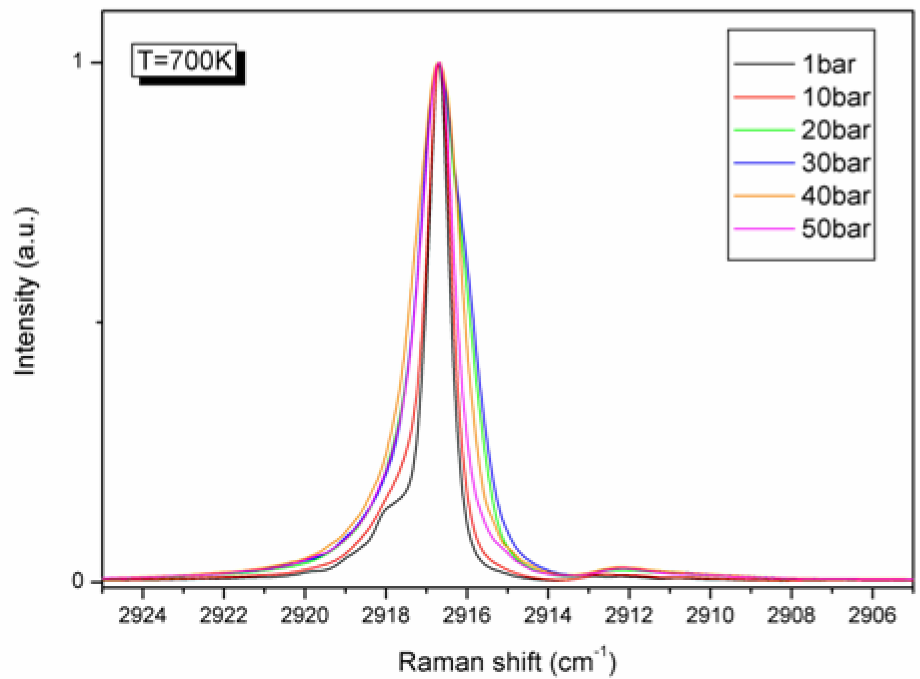

Pressure effect

ONERA

CARS in Practical kerosene/air Combustors

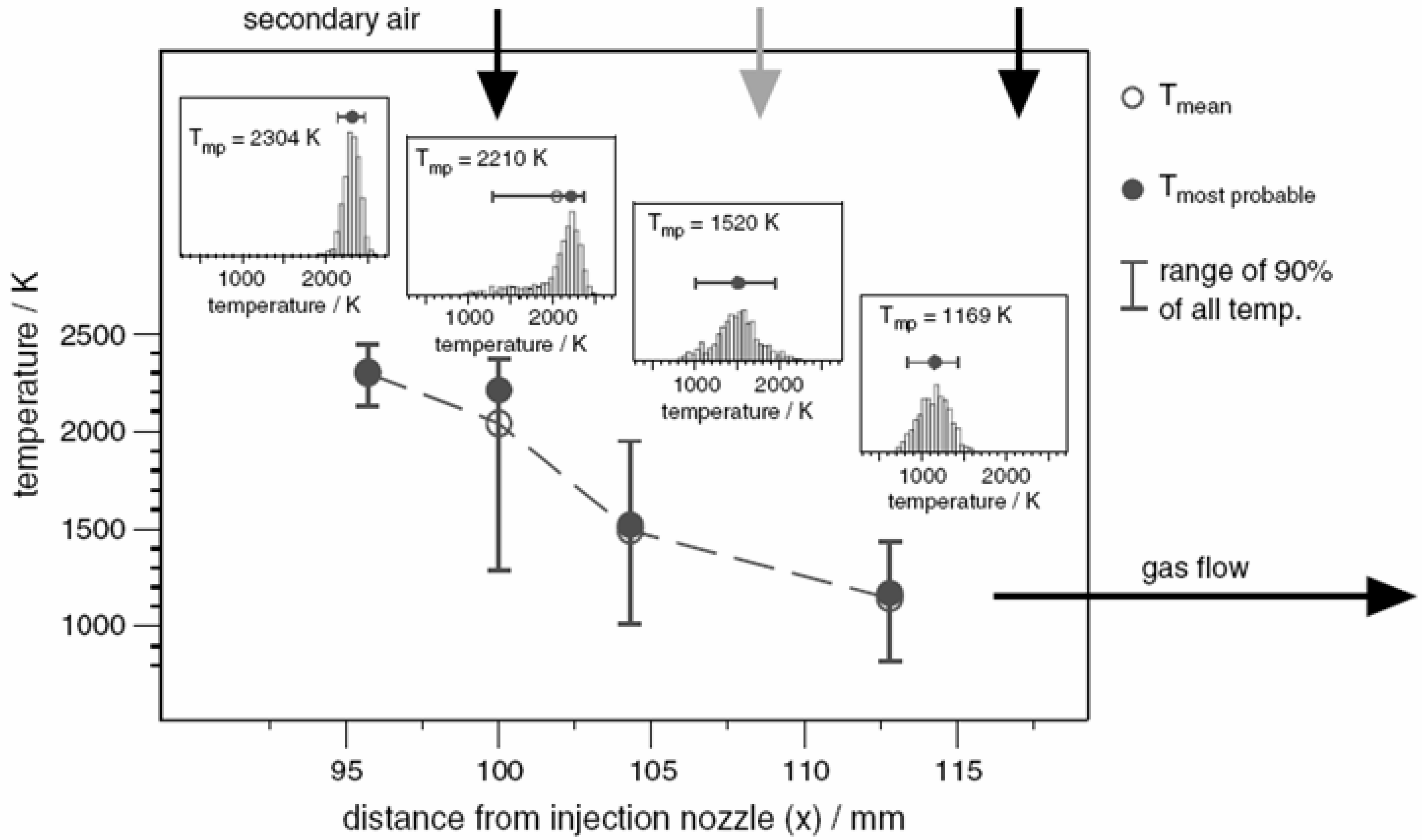

Figure 4. Axial temperature profile in the quench region of the kerosene-fuelled RQL combustor at atmospheric pressure. The data points were taken in a plane below a row of secondary air holes.

Stricker et al., J. Raman Spectroscopy, Vol. 34, 922 (2004) (DLR experiment).

CARS in Practical kerosene/air Combustors

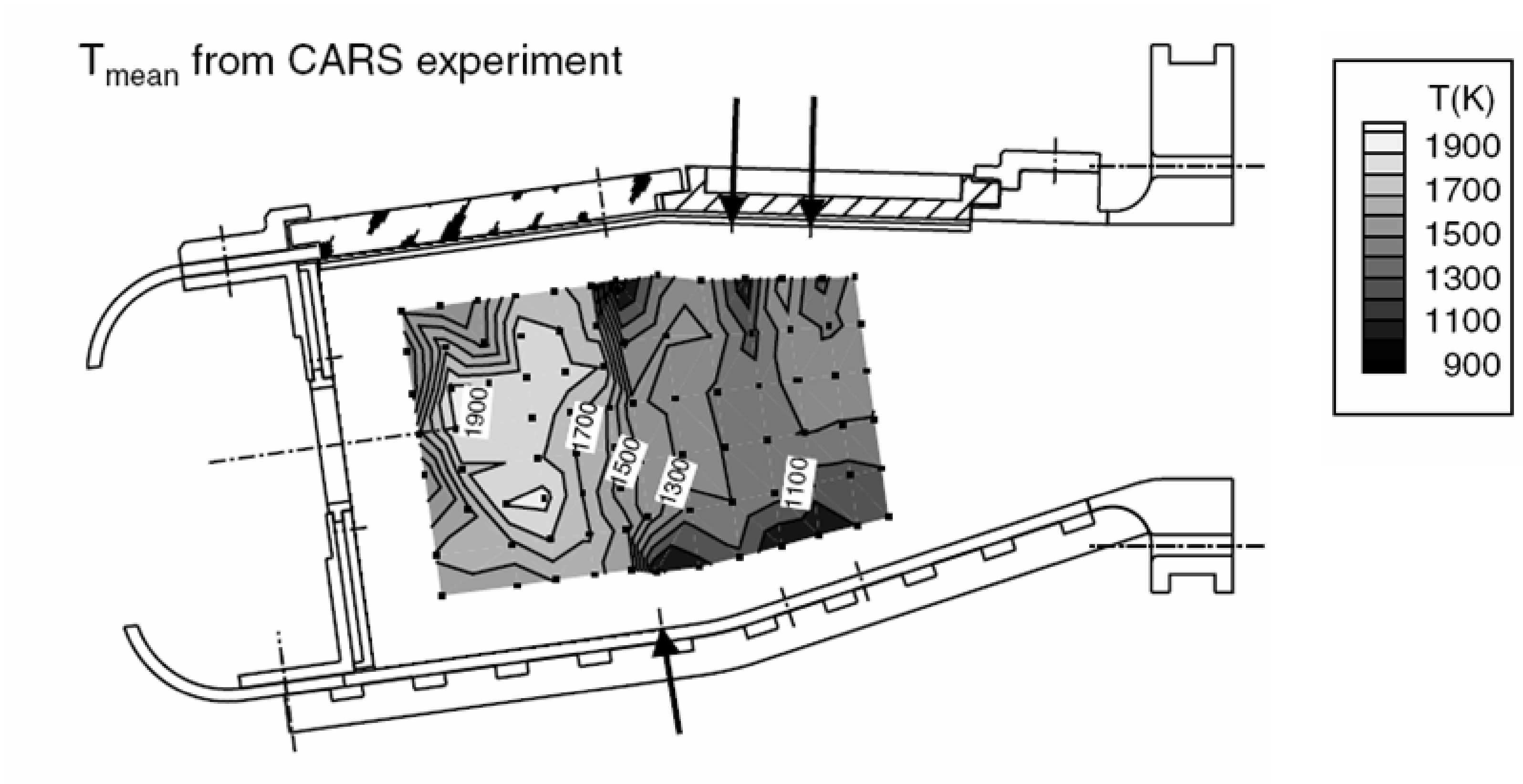

Stricker et al., J. Raman Spectroscopy, Vol. 34, 922 (2004).

- Same experiments performed at ONERA on a multi-point injection system at pressure up to 19 bar (TLC European Research Program)

HYPERSONICS STUDIES

LBK wind tunnel

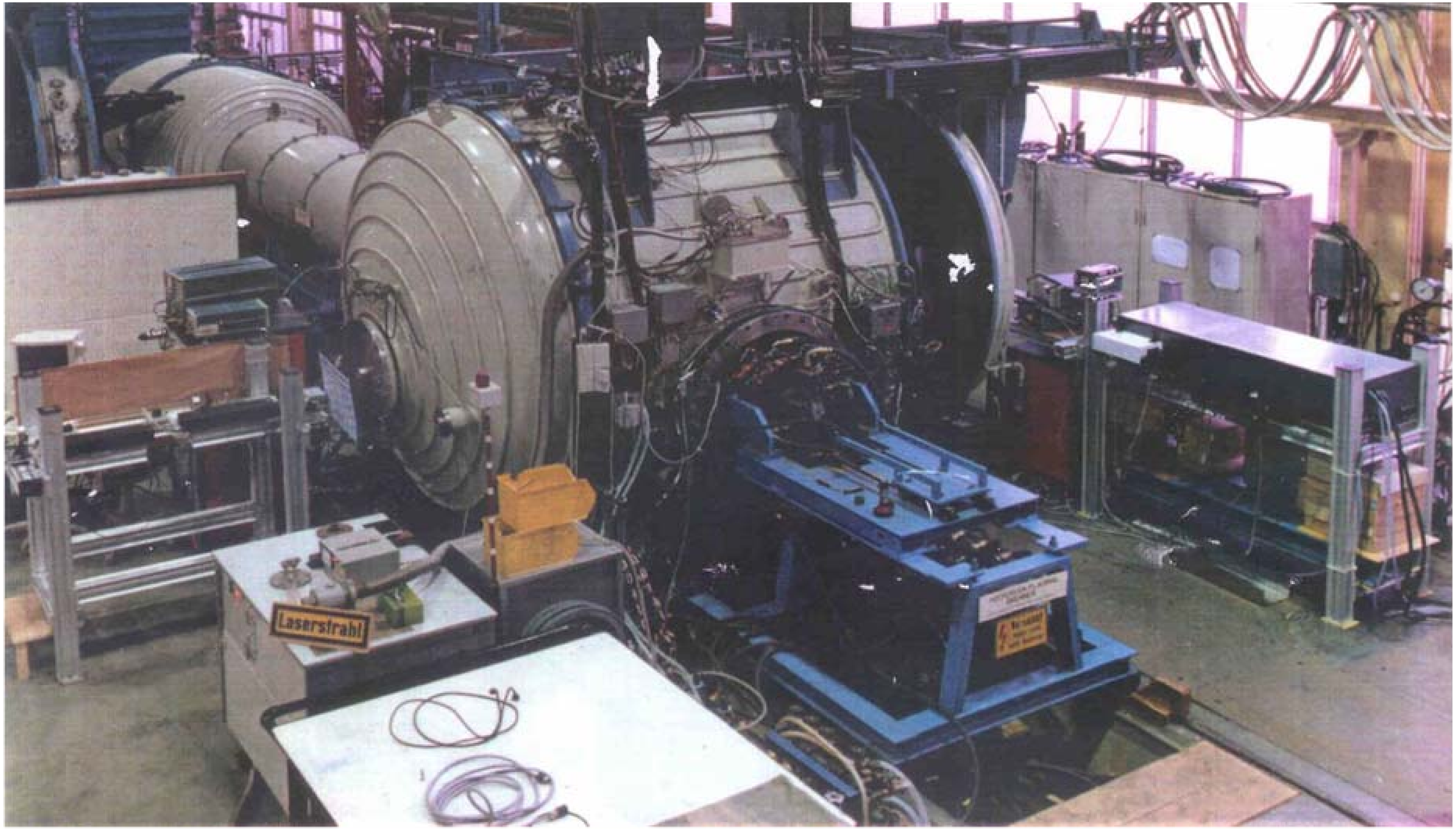

ONERA

Experimental set-up

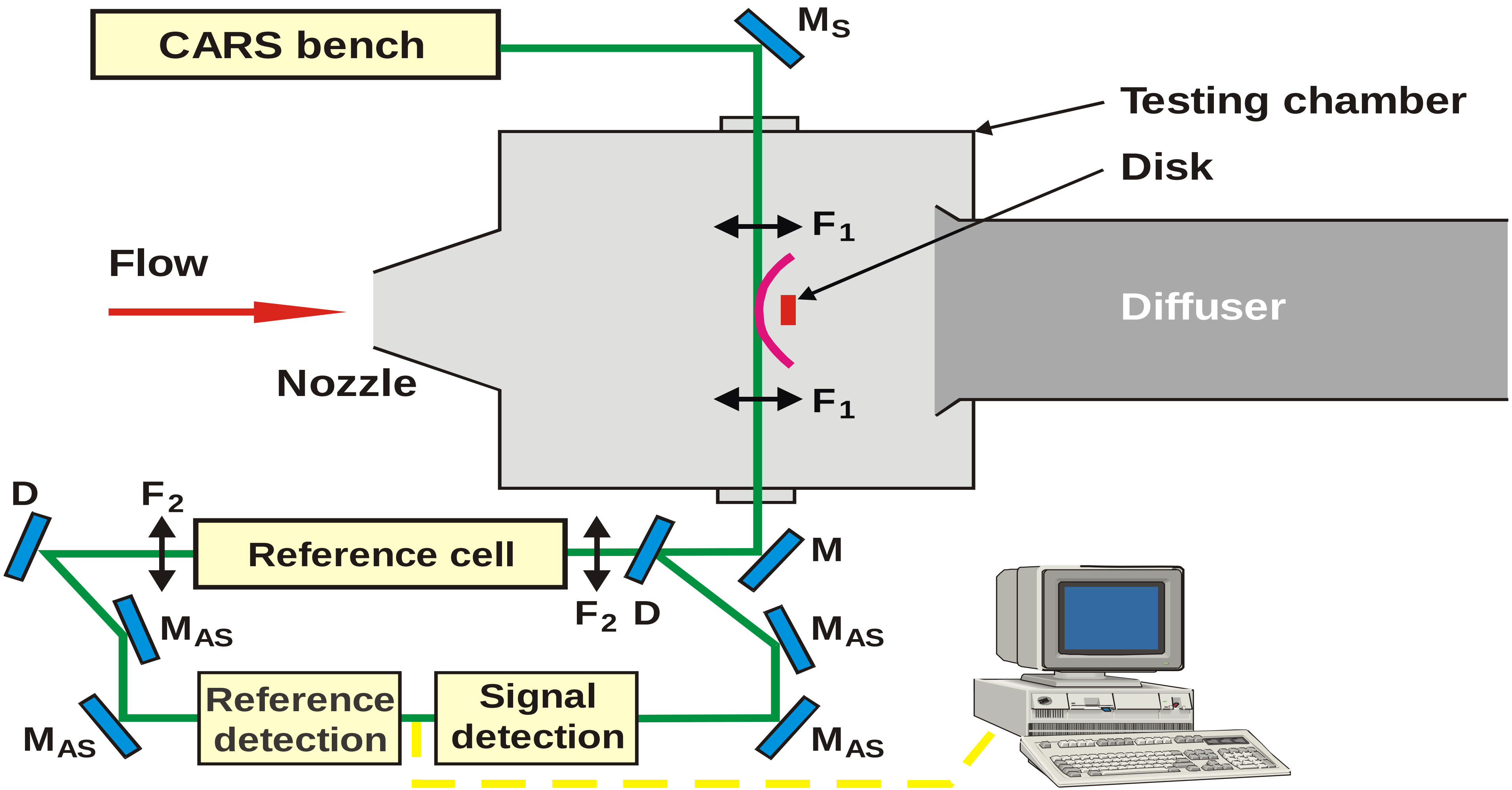

Probe volume : 20 mm-long x 100 μm in diameter

LBK wind tunnel

- **Stagnation conditions**

Air

Gas flow rate :	**49 g/s**
Pressure :	**1.3 bar**
Total enthalpy :	**7.3 MJ/kg**
Temperature :	**3910 K**

- **Conical Nozzle**

Throat diameter :	**29 mm**
Exit diameter :	**200 mm**
Length :	**405 mm**

- **Conditions at the probe volume (995 mm from the throat)**

Mach number :	**7.5**
Static pressure :	**14 Pa**

Shock layer on disk at LBK

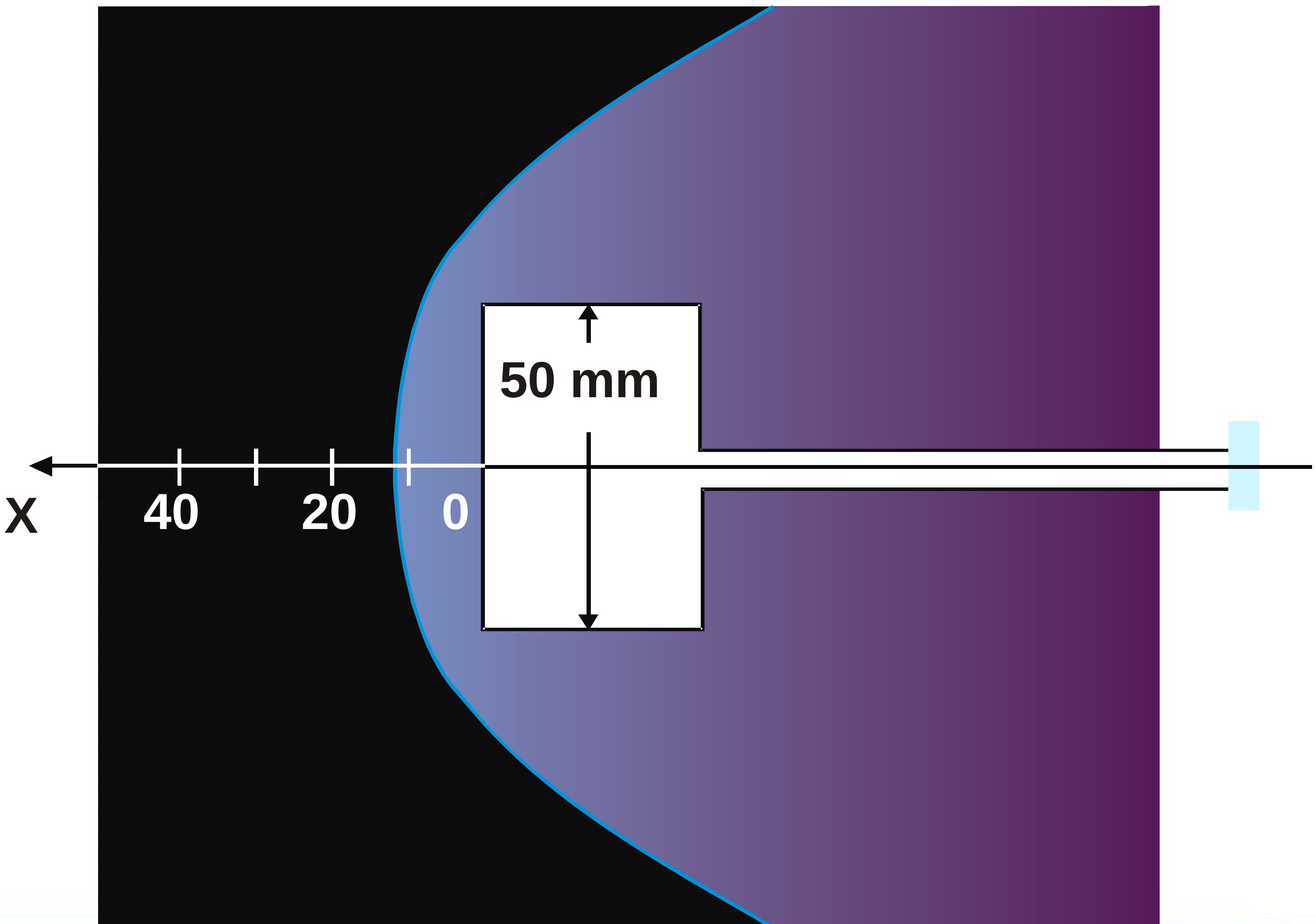

L2K Free Stream

Temperature measurement with CARS

N$_2$ CARS Spectrum

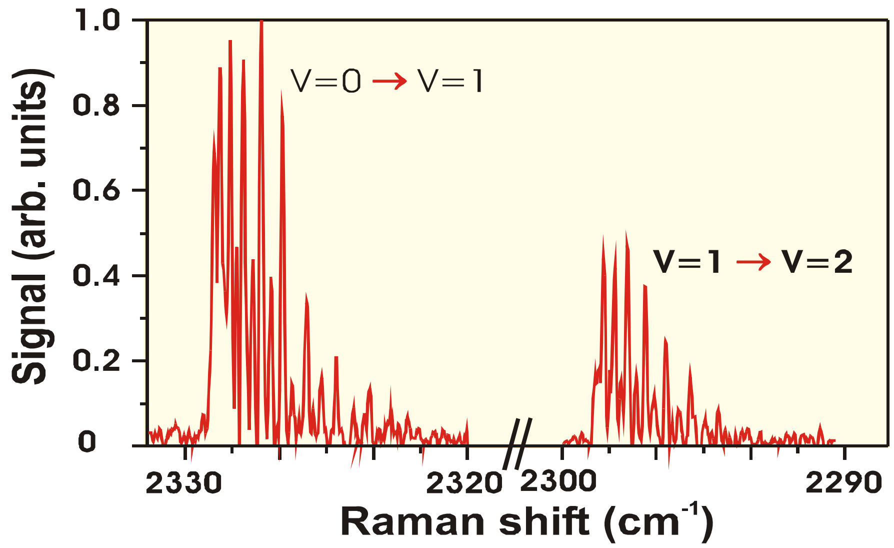

Boltzmann Diagram

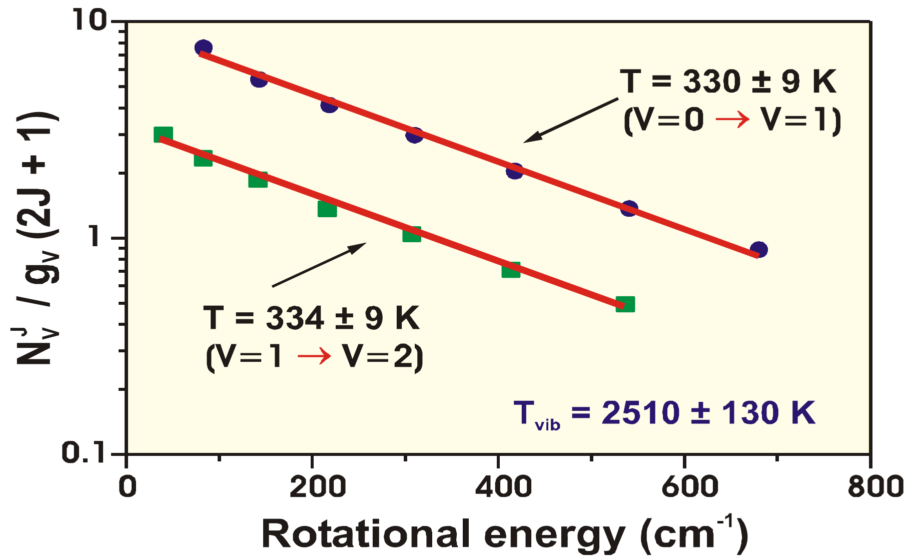

Nitrogen CARS spectra

Free stream

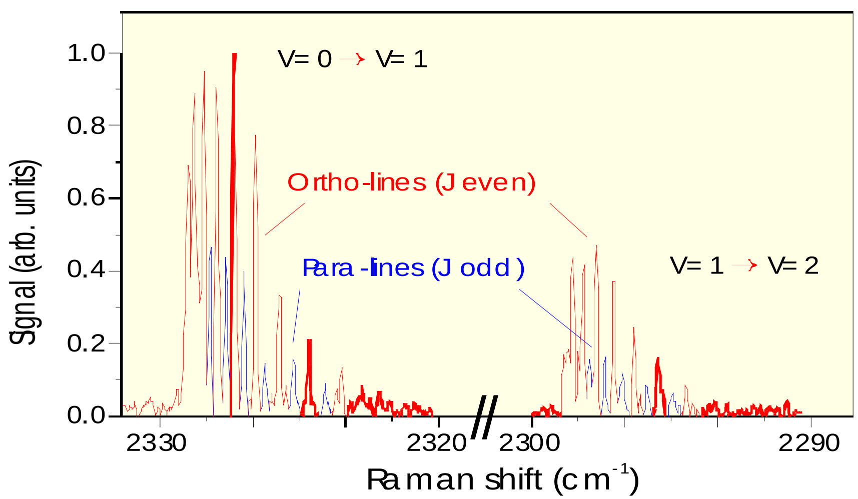

Shock layer

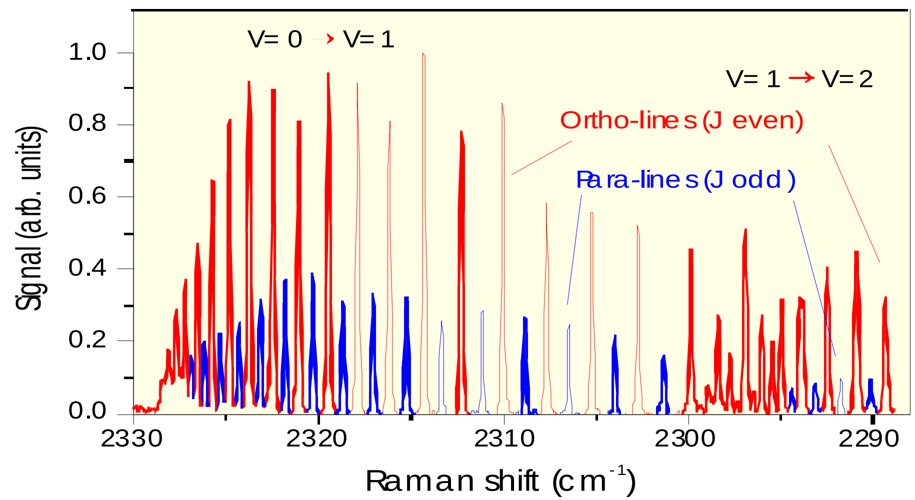

Temperature Distributions in the Shock Layer

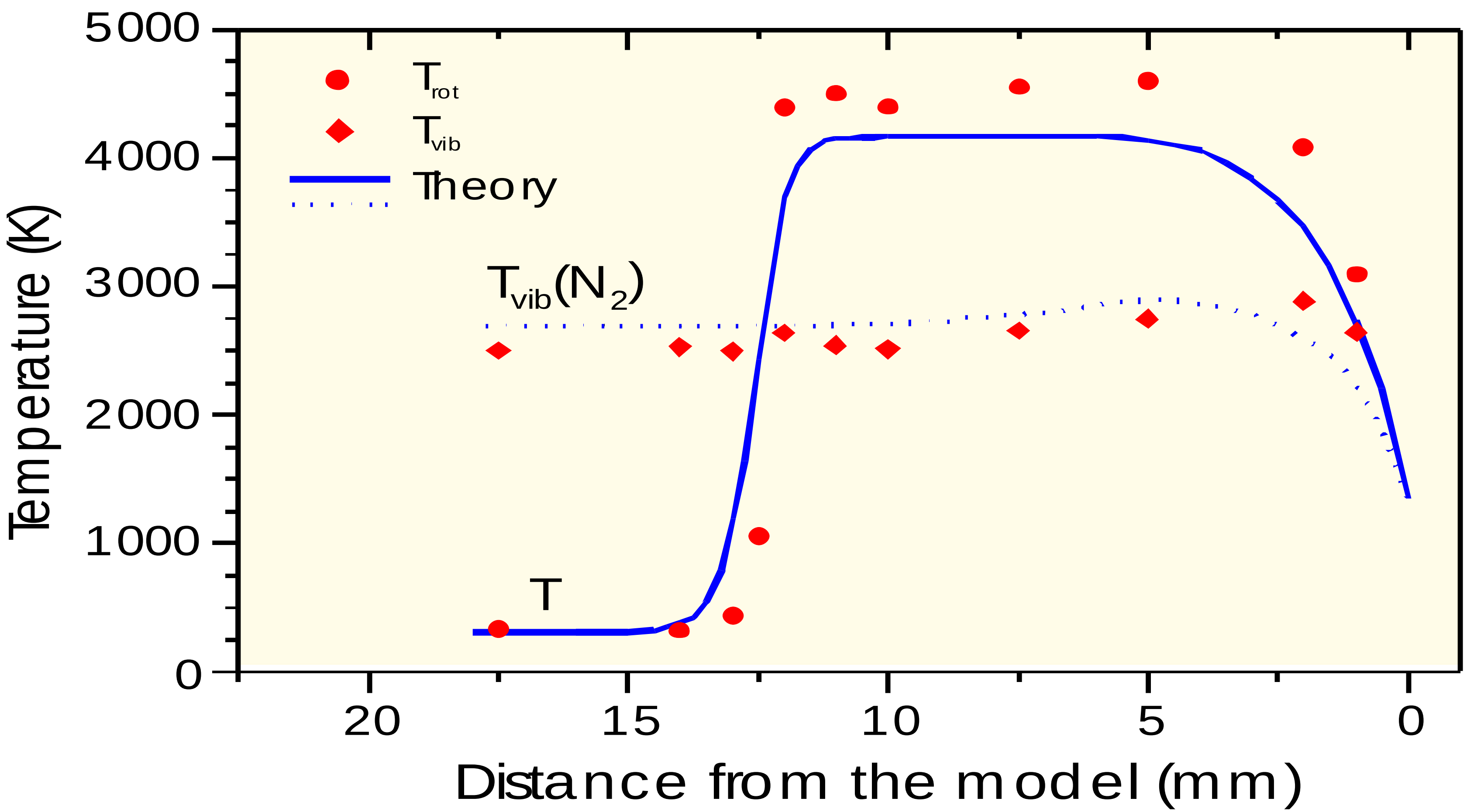

ONERA

Density Profile in the Shock Layer

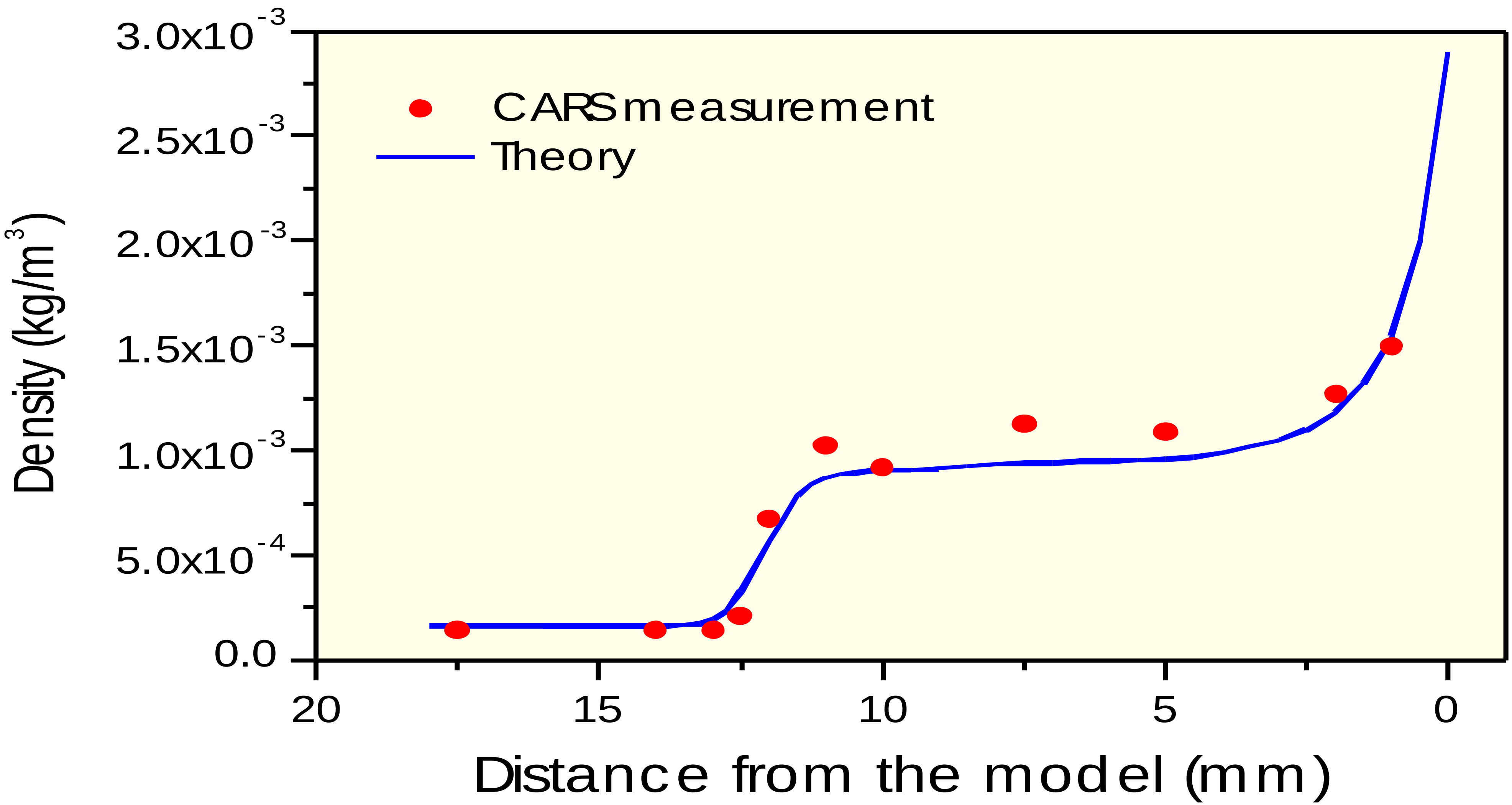

Coherent anti-Stokes Raman Scattering in the time domain

Office National d'Études
et de Recherches Aérospatiales

Velocity measurements by time-domain CARS

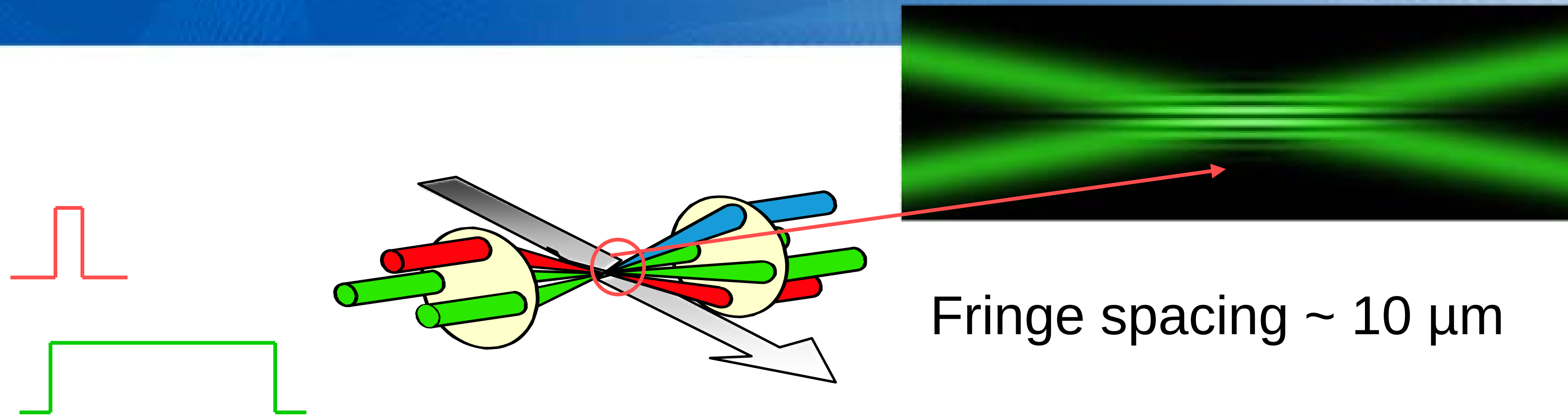

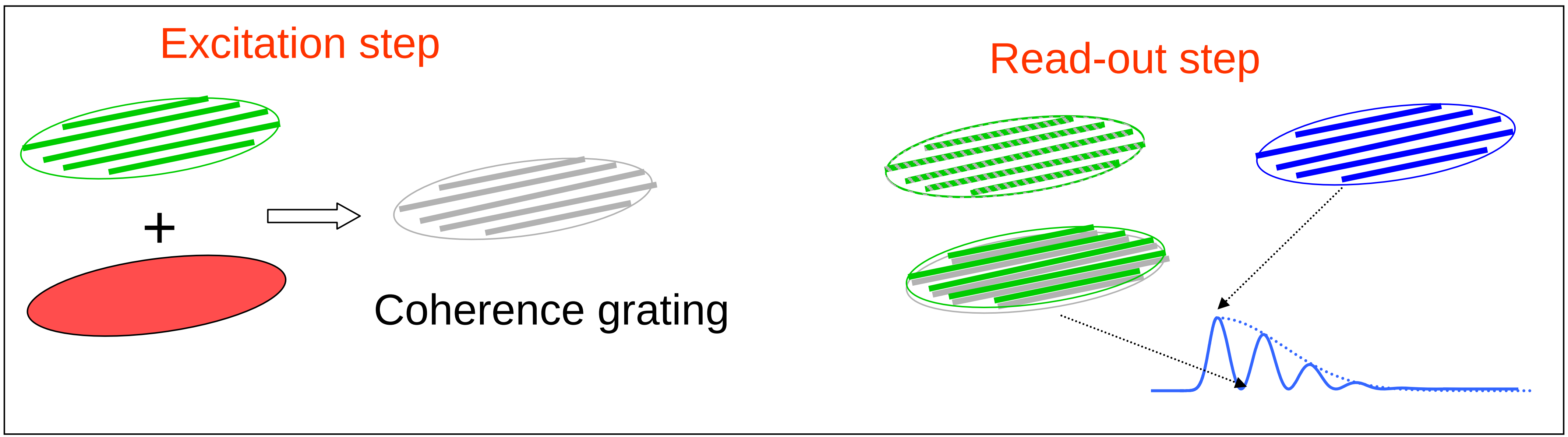

Ribet I., Scherrer B., Bouchardy P., Pot T., Taran J.-P., Lefebvre M.
Supersonic flow diagnostics by single-shot time-domain CARS
J. Raman Spectrosc., **31**, 689 (2000)

Experimental set-up

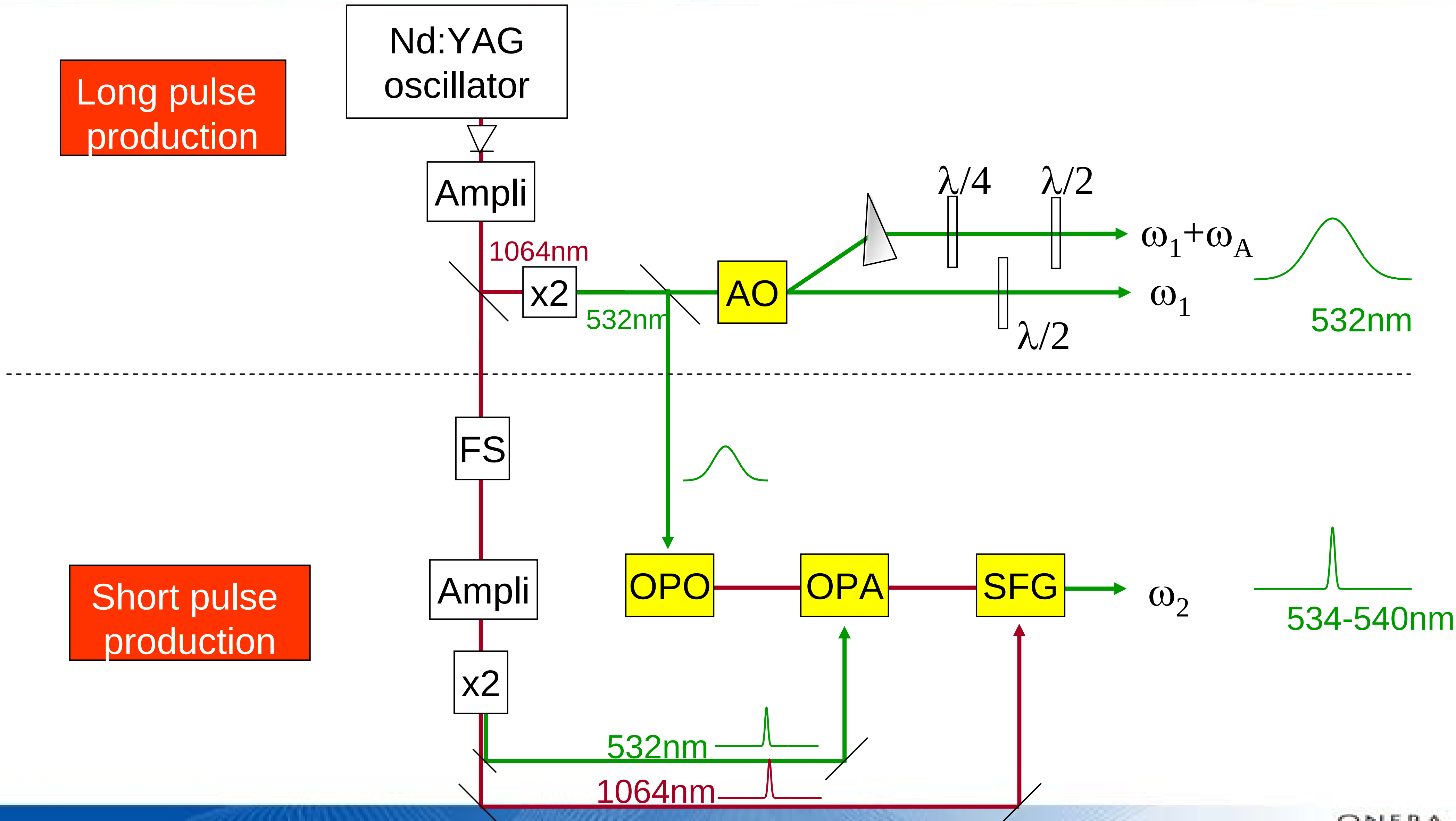

Velocity measurements (free stream)

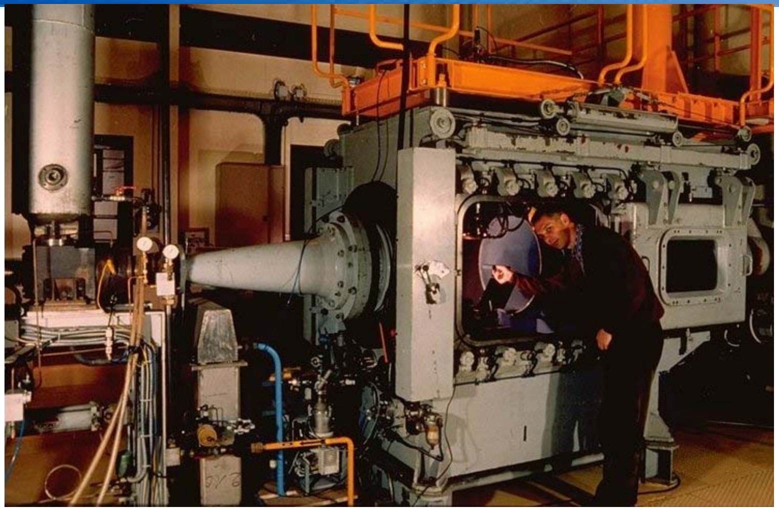

R5 wind tunnel (Mach 10)

Heater ON

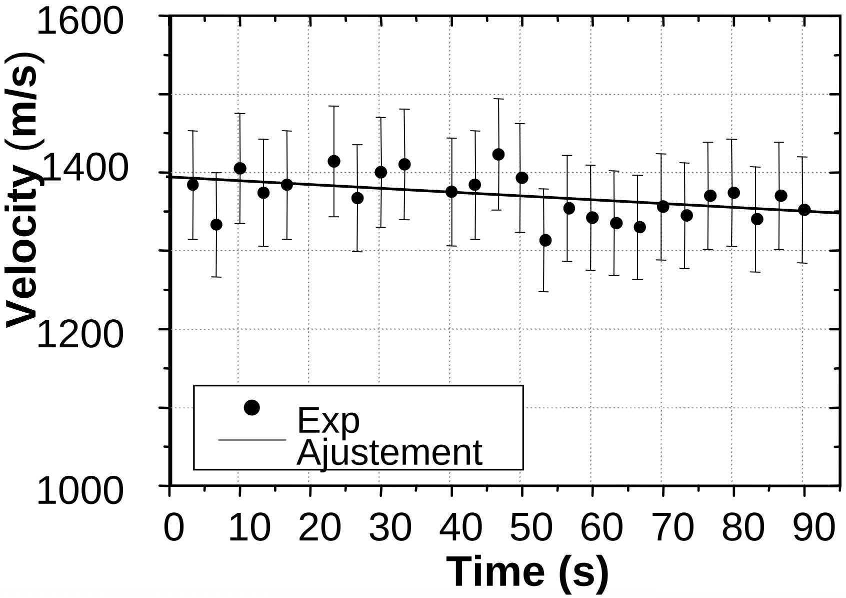

Heater OFF

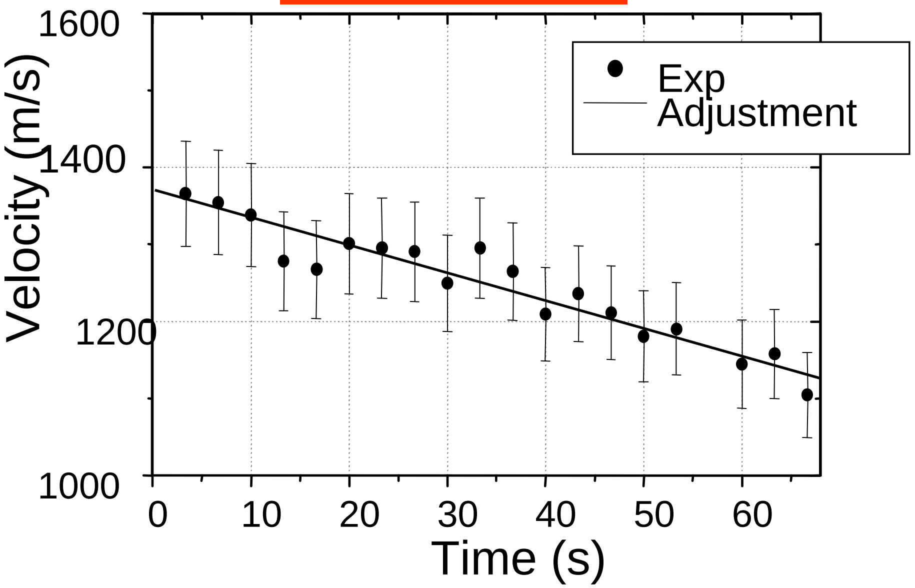

Velocity, temperature and density in bow shock

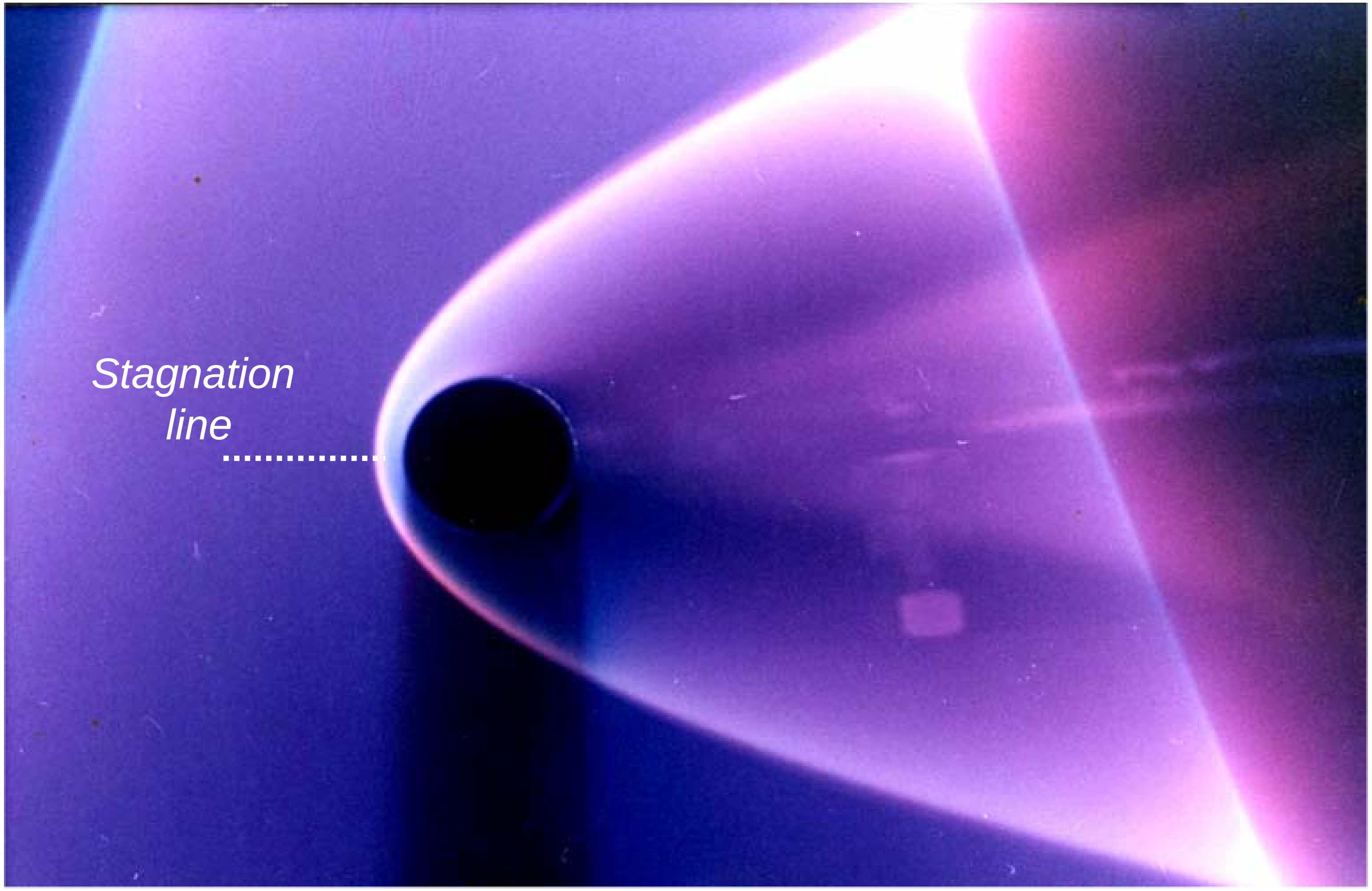

Molecular degrees of freedom through the shock

Boltzmann diagram

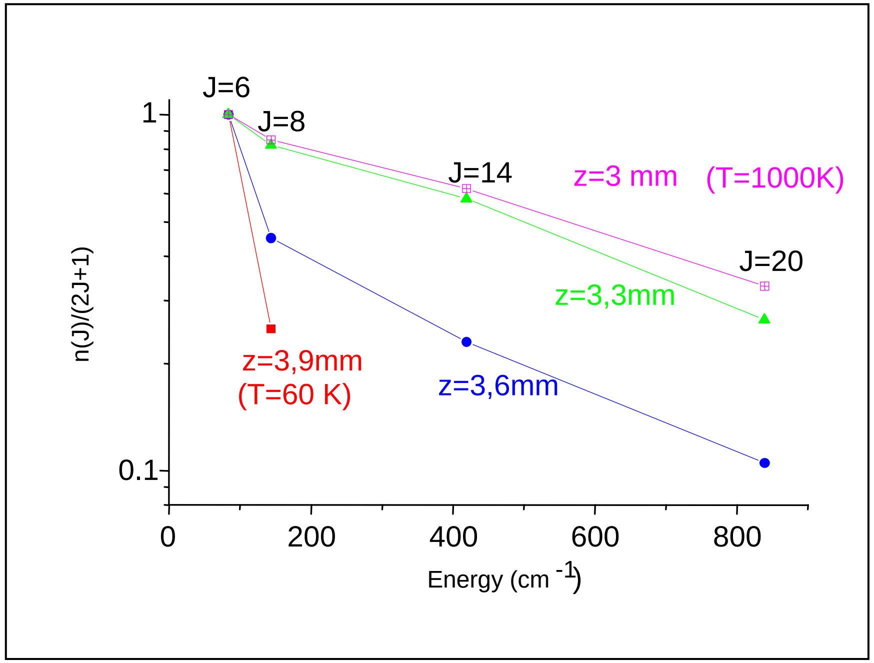

Static temperature and velocity

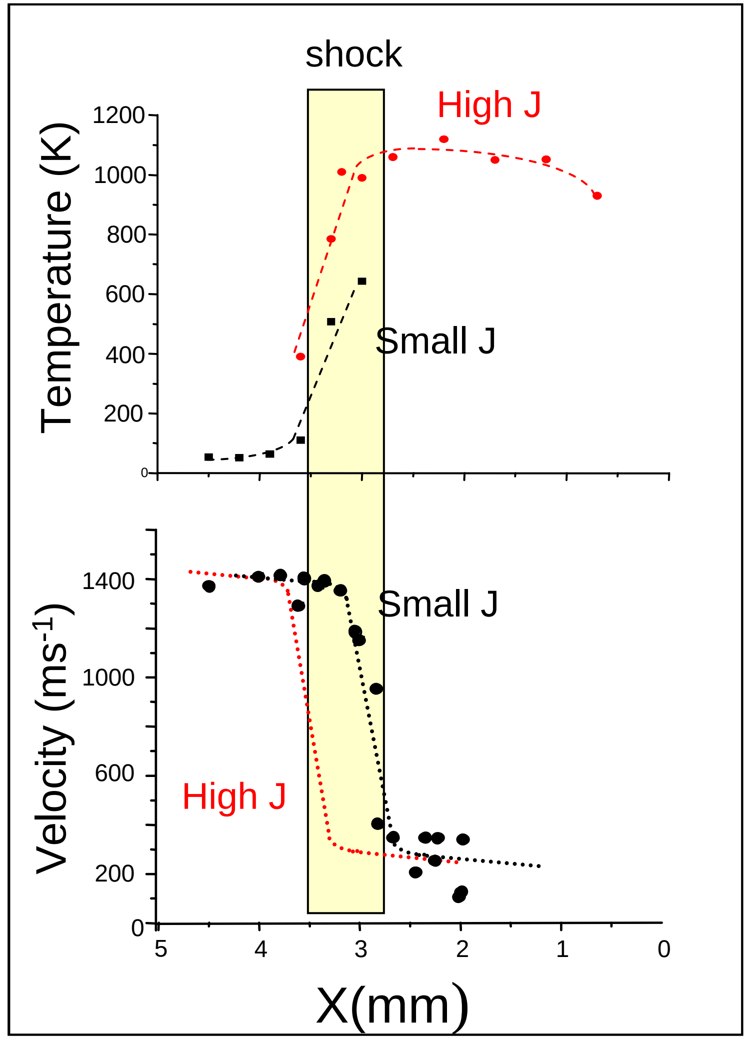

Velocity measurements above a flat plate

100 mm downstream the leading edge

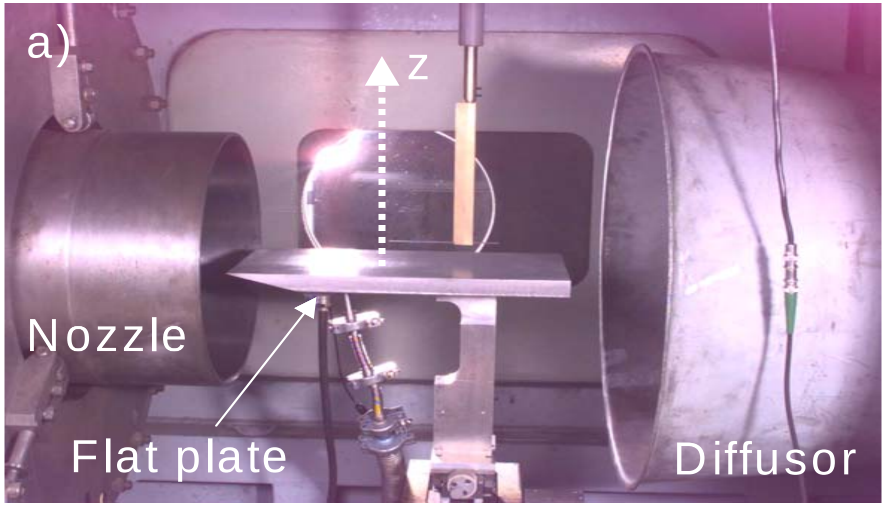

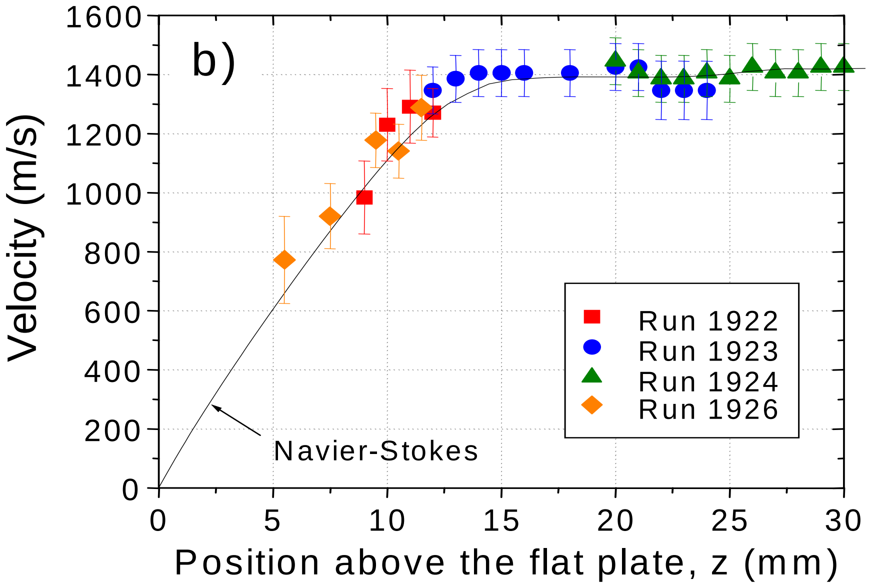

OTHER NON-EQULIBRIUM MEDIA

- Low-pressure discharges
  - H_2, N_2, O_2, etc.
- Photochemistry
  - H_2CO (Moore)
- Explosives
  - Lead azide (Rosenwaks)

RESONANCE-ENHANCED CARS

- Druet, Attal-Trétout, with
  - Gustafson,
  - Bordé,
  - Dumont,
  - Kelley,
  - etc.

CONCLUSION

- **I – with CARS, we have witnessed a remarkably productive cross fertilisation between laser optics and molecular physics**

- **II – hypersonics is, really, a problem in quantum mechanics**